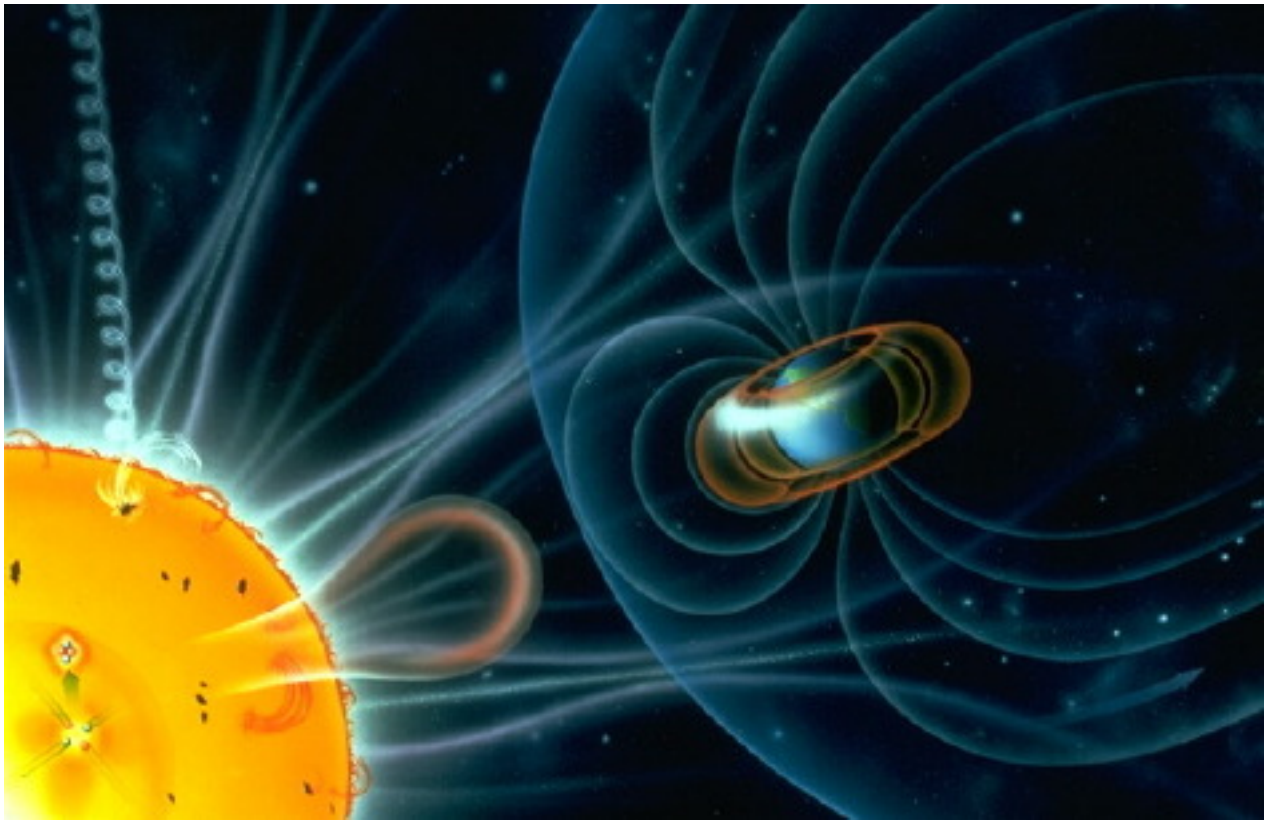

Geomagnetic Storms and Substorms

F. Toffoletto, Rice University

With thanks to R. A. Wolf, Rice U.

Outline

- Geomagnetic Storms
  - Basic properties of a geomagnetic storm
  - Basic features of the Inner magnetosphere and ring current during a storm
  - Storm simulations with a ring current model (RCM)
- Substorms
  - Basic properties of a substorm
  - Various Substorm Models
    - Relationship to CME models?
    - Pressure balance inconsistency
  - Relationship to storms
- Summary

Magnetic Storms

- Dst is a measure of the deviation of H (north-south) component of the magnetic field near the Earth's equator from a long term average
- The diagram below represents an ideal magnetic storm, which has all four phases.
  - The main phase is the defining feature of a storm. The main phase represents ring-current injection, which results from a southward IMF and the resultant strong convection.
  - Some storms have no sudden commencement.
  - Some storms have a sudden commencement but no initial phase: in that case, the main phase begins immediately after the compression.
  - The recovery phase is due to loss of ring-current ions as a result of charge exchange with the neutral exosphere.

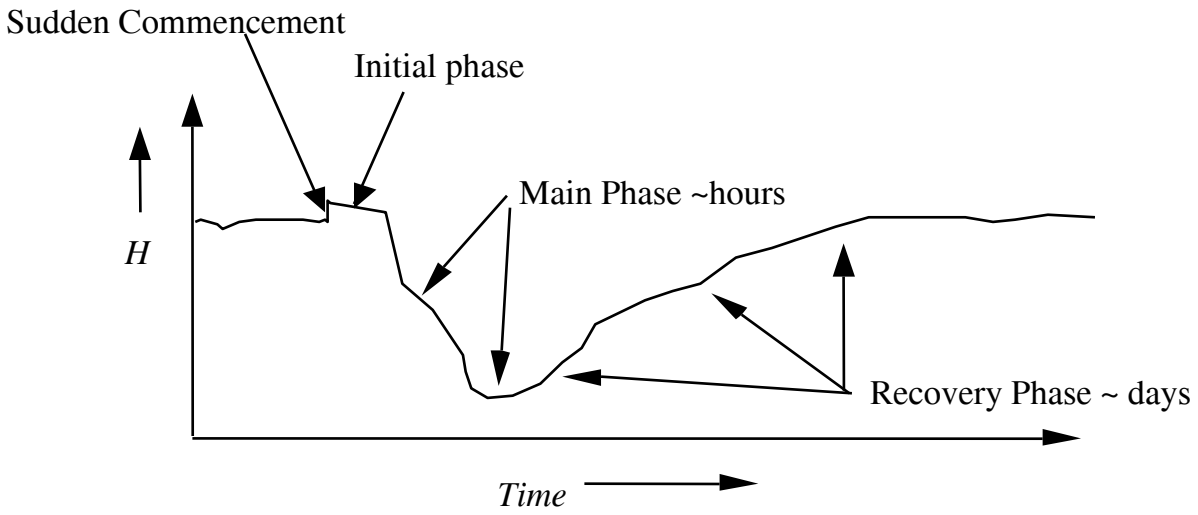

Magnetic Cloud Events

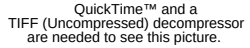

Figure from Tsurutani et al, JGR 2003

- Most very large magnetic storms on Earth are caused by magnetic clouds or “islands.”
  - Strong organized magnetic field
  - Long period of northward field and long period of southward field.
    - Southward field causes storm

Question

- The sudden commencement of a storm (as seen in the Dst becoming positive) usually associated with the arrival of a shock in the solar wind
  - Why?

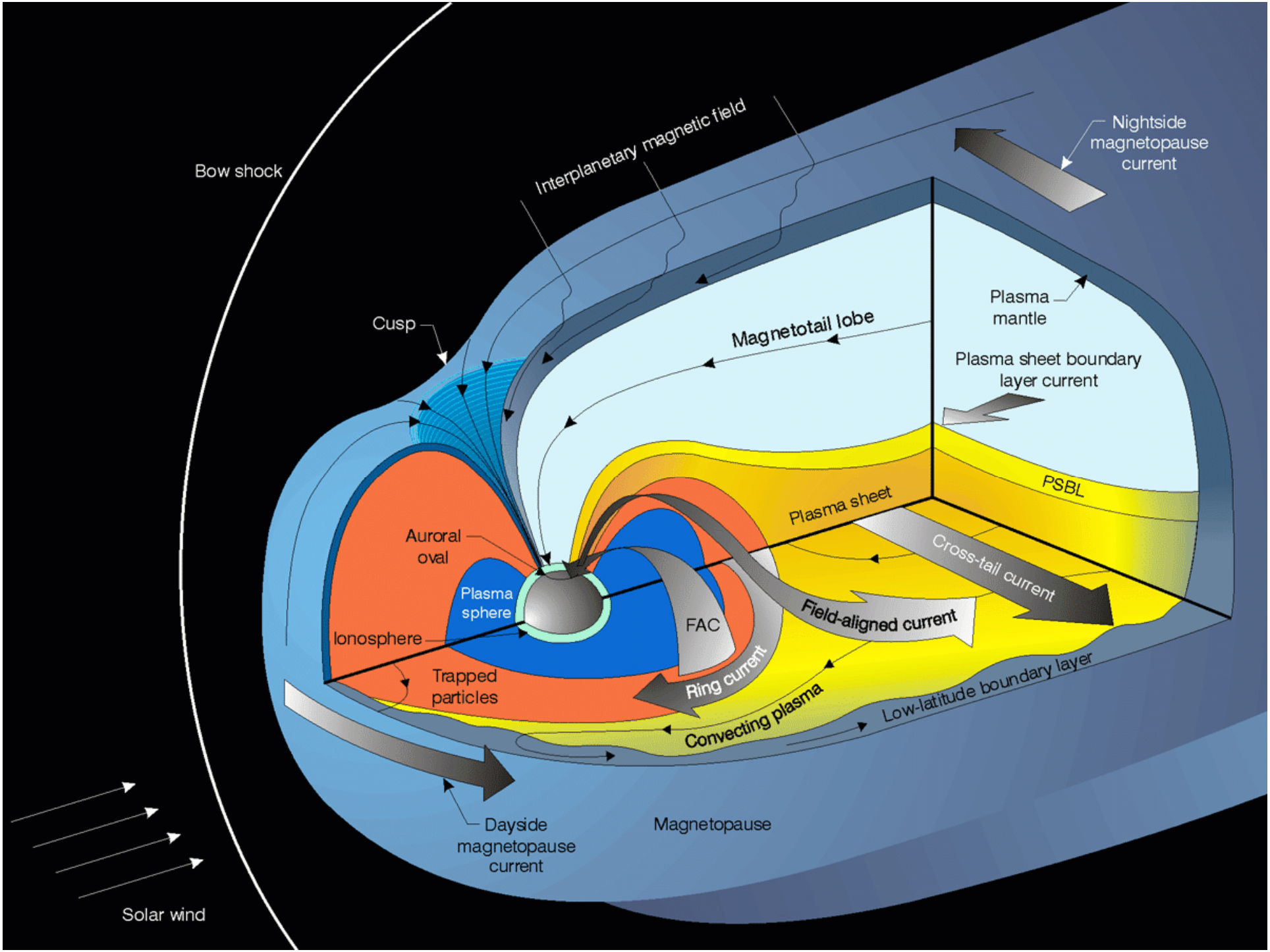
Bow shock
Interplanetary magnetic field
Nightside magnetopause current
Cusp
Magnetotail lobe
Plasma mantle
Plasma sheet boundary layer current
PSBL
Plasma sheet
Auroral oval
Plasma sphere
Ionosphere
Trapped particles
FAC
Field-aligned current
Cross-tail current
Ring current
Convecting plasma
Low-latitude boundary layer
Dayside magnetopause current
Magnetopause
Solar wind

Dst occurrence frequency

Dst Range (nT)	Occurrence Frequency
50 - 150	monthly
150-300	Few times / year
>500	Few times solar cycle

Carrington, 1859 Storm

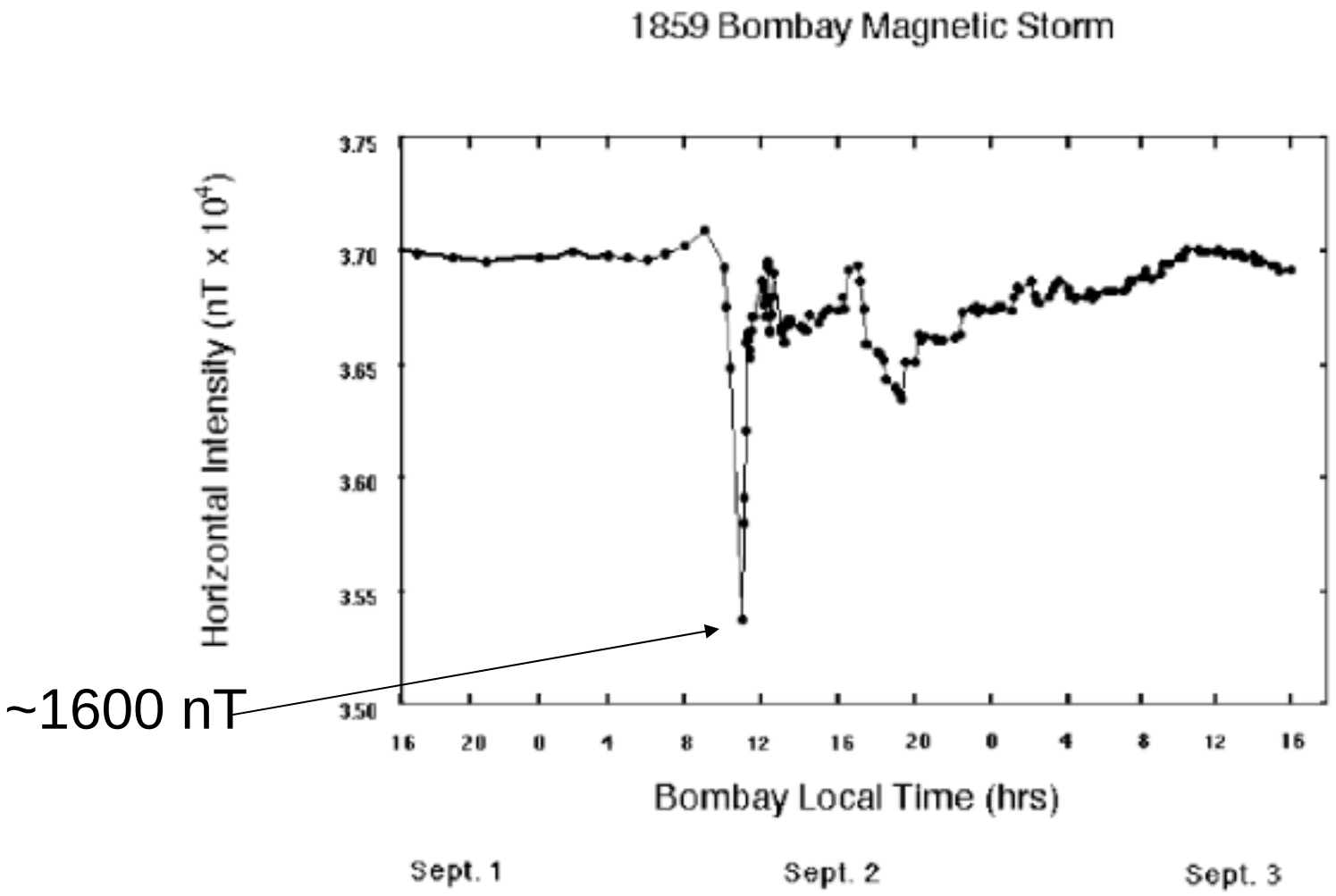

From Tsurutani et al, JGR 2003

Question

- What current systems can be associated with the southward excursion of Dst?

The Ring Current

- Definition:
  - The *ring current* consists of particle populations that are in trapped orbits about the Earth and have sufficient energy to carry substantial current and affect the magnetic field.
    - Basically ions with energies between about 10 keV and about 200 keV.
    - More energetic ions have small enough number density that they don't contribute significantly to the macroscopic current.
    - Electrons in the same energy range are insufficiently numerous to carry significant current.

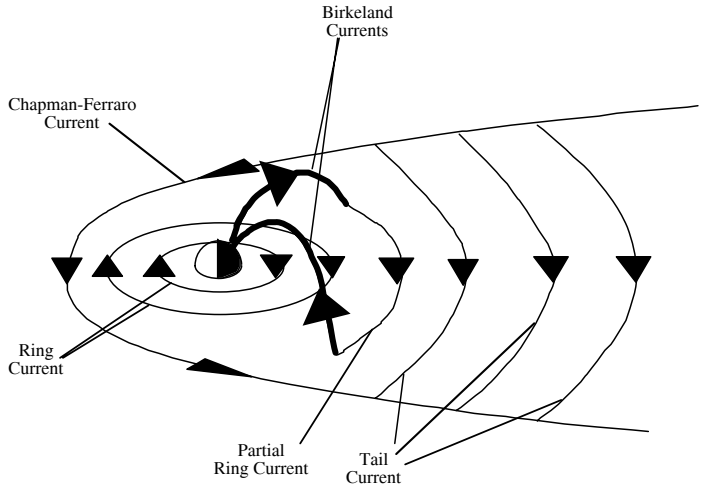

The Inner Magnetosphere - particle populations

- There are no sharp distinctions among the terms *radiation belt*, *plasmasphere*, and *ring current*, because there are no sharp physical divisions in the particle populations themselves.
- The *plasmasphere*, which consists of particles of relatively high density (10-10^3 cm^{-3}) and low energy (usually less than 1 eV). This population decreases outwards and terminates at a boundary called the *plasmapause*, which is usually relatively sharp.
- Although particles of almost all energies contribute to the ring current, the name *ring current particles* is typically applied to particles with energies between a few keV and ~ 200 keV.
- The names *radiation belt*, or *Van Allen belt*, are usually applied to particles with energies between ~ 40 keV and a few hundred MeV. These particles, though too small in number to be a major element in the overall dynamics of the magnetosphere, were discovered first, because they existed at low altitudes and could be detected by a simple Geiger tube.

Quiet-Time and Storm-Time Ring-Current Distribution

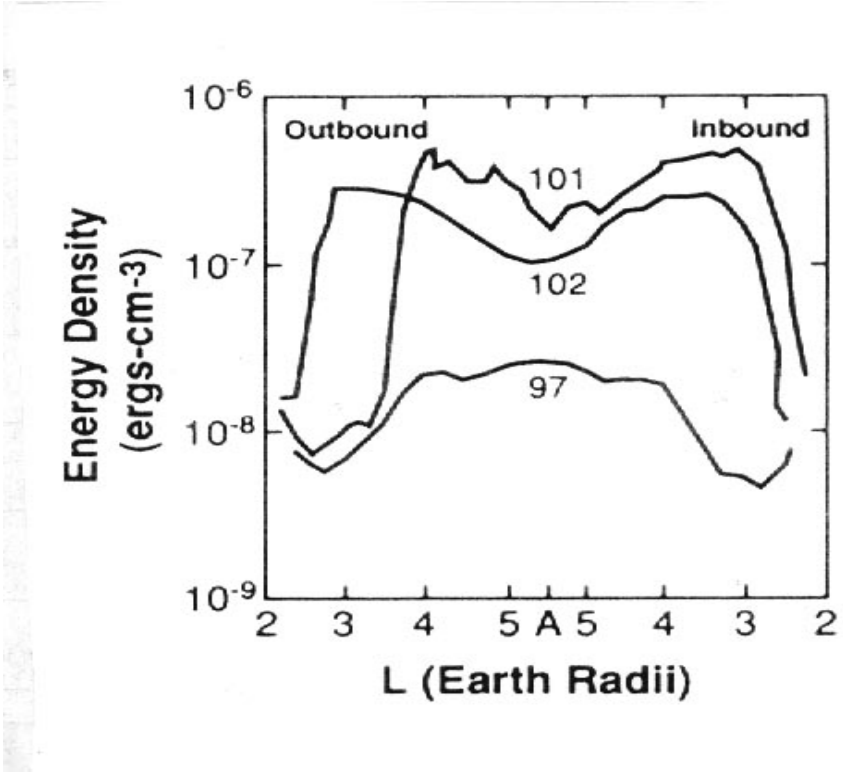

Orbit 97 took place before the storm and represents the quiet-time ring current. Orbit 101 took place in the early recovery phase, orbit 102 in the late recovery phase. Adapted from Smith and Hoffman (*JGR*, *78*, 4731, 1973).

- Note:
  - Particle energy density increases more than an order of magnitude in the storm.
  - Little increase for $L<2.5$.

Quiet-Time and Storm-Time Ring-Current Particle Energy Spectra

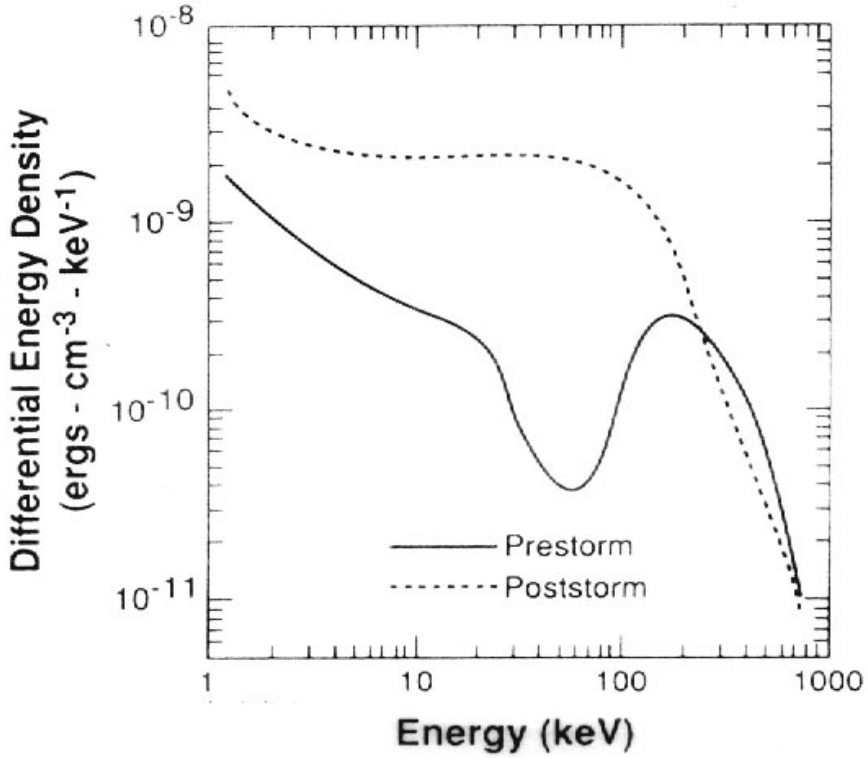

Differential energy density in ring current ions Adapted from Smith and Hoffman (1973).

- The flux of ring-current ions increases in the storm from 1 keV to about 200 keV.

Ring Current Composition

AMPTE measurements of ring current in storm of September 5, 1985. From Gloeckler and Hamilton (*Phys. Scripta*, 18, 73, 1987).

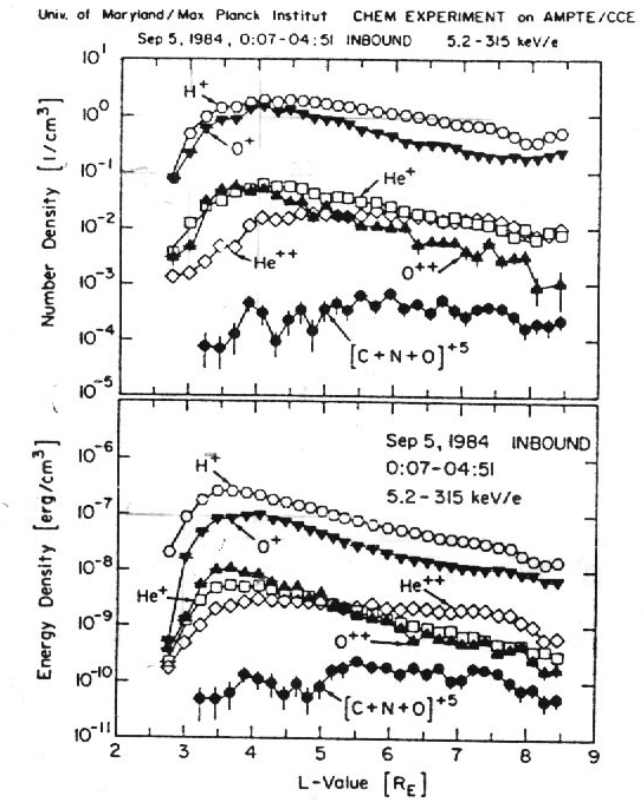

- Although everybody had expected that the ring current was made of protons, the first composition measurements (made in the mid-1980's from the AMPTE-CCE spacecraft) showed that O^+ was a major component.
- H+ dominates above about 100 keV. O+ dominates below 15 keV.

Magnetic Storms

- Dst is a measure of the deviation of H (northward) component of the magnetic field near the Earth's equator from a long term average
- The diagram below represents an ideal magnetic storm, which has all four phases.
  - The main phase is the defining feature of a storm. The main phase represents ring-current injection, which results from a southward IMF and the resultant strong convection.
  - Some storms have no sudden commencement.
  - Some storms have a sudden commencement but no initial phase: in that case, the main phase begins immediately after the compression.
  - The recovery phase is due to loss of ring-current ions as a result of charge exchange with the neutral exosphere.

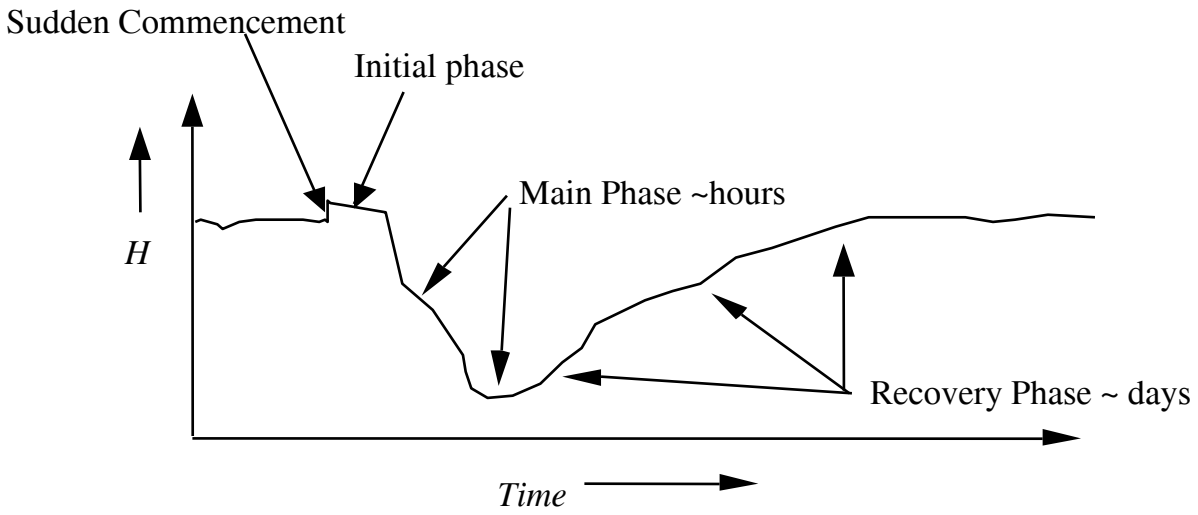

Charge Exchange

- The uppermost part of Earth's neutral atmosphere is the exosphere, consisting of particles on ballistic orbits
  - Above ~ 1000 km altitude, collision mean free path exceeds the scale height.
  - Neutral particles (mostly H) follow elliptic trajectories
- Charge exchange reactions between ring current ions and exospheric neutrals
  - $H^+(keV)+H(<1eV) \rightarrow H^+(<1eV)+H(keV)$
  - $O^+(keV)+H(<1eV) \rightarrow H^+(<1eV)+O(keV)$
  - The kilovolt neutral goes off in a straight line, because its kinetic energy is thousands of times the gravitational binding energy.
    - Sometimes plunges into the lower atmosphere
    - Usually escapes into space
    - In either case, the kilovolt particle's energy is lost to the magnetosphere.
  - The < 1 eV ion becomes part of the cold-plasma population, similar to the plasmasphere.
    - Doesn't contribute significantly to the gradient/curvature current or to the pressure.

Neutral-Atom Imaging

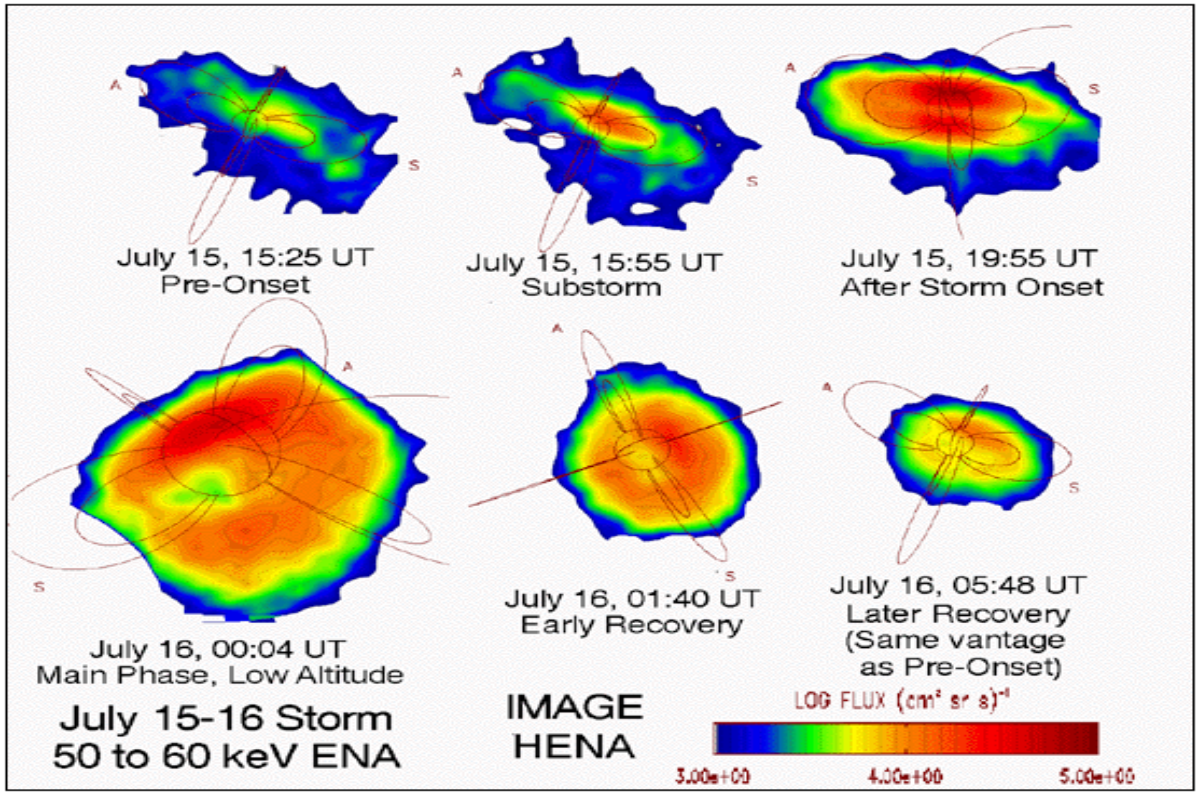

Neutral atom image of the July 15-16 storm (50-60 keV neutrals). From IMAGE spacecraft web page.

Loss by Coulomb Scattering

- When ring current ions lie within the plasmasphere, they lose energy by repeated Coulomb collisions with the cold electrons of the plasmasphere.
- They also heat the plasmaspheric electrons.
  - Contribute to the subauroral red arc (SAR arc) phenomenon.

Ring Current Lifetimes

- For H^+ and O^+, Coulomb scattering is dominant mostly for ions less than about 10 keV.
  - Ionization potentials are almost the same for H^+ and O^+.
- For He^+, charge exchange lifetimes are longer, and Coulomb scattering more important.
  - However, He^+ is a minor component of the ring current.
- Below about 50 keV
  - Charge exchange lifetimes are less than a day for H^+
  - Charge exchange lifetimes are mostly > 1 day for O^+ in this energy range.
  - That is why O^+ tends to dominate the energy density below about 50 keV.
- Above about 50 keV
  - Hydrogen lifetimes get long
  - O+ charge exchange lifetimes become short.
  - That is why H^+ tends to dominate the ring current above about 50 keV.

Modeling Storms with the RCM - Introduction

- The Rice Convection Model (RCM) is based on the elegant and well-developed theory of adiabatic particle motion for the inner and middle magnetosphere
  - Applicable to the quasi-dipolar part of the magnetosphere (<10 R_E)
    - In regions where flow speeds are slow compared to the thermal speeds
  - Can also be applied to the middle plasma sheet out to ~30 R_E
- Most of the important particle populations of the magnetosphere, and particularly the ones that carry most of the pressure, energy, and current, are non-relativistic.
- Since energy dependent gradient and curvature drifts become important in the inner region, MHD is not applicable.

RCM Transport Equations

- Take an isotropic distribution function and "slice" it into "invariant energy" channels:

$$\lambda_s = W_s V^{2/3}(\vec{x}) \quad \text{where} \quad V(\vec{x}) = \int_{fieldline} \frac{ds}{B}$$

- Specific Entropy $pV^{\gamma} = \frac{2}{3}\sum_s |\lambda_s|\eta_s$

- For each "channel", transport is via an advection equation:

$$\left(\frac{\partial}{\partial t} + \vec{V}_D(\lambda, \vec{x}, t)\cdot\nabla_2\right)\eta_s(\vec{x},t) = -\frac{\eta_s(\vec{x},t)}{\tau_s(\vec{x},t)}$$

$$\vec{V}_D(\lambda,\vec{x},t) = \frac{\vec{E}(\vec{x},t)\times\vec{B}(\vec{x},t)}{B(\vec{x},t)^2} + \frac{\vec{B}(\vec{x},t)\times\nabla W(\lambda,\vec{x},t)}{qB(\vec{x},t)^2}$$

- These fluids (typically around 100, including ions and electrons) are tracked in the RCM
- Without losses, the specific entropy of each fluid is conserved along a drift path $(pV)^{\gamma}_s = \frac{2}{3}|\lambda_s|\eta_s$
- *Reference: Wolf, in Solar-Terrestrial Physics, ed. Carovillano and Forbes, 1983.*

Determining the Inner Magnetospheric electric field

- Vasyliunas equation in MHD form (comes from neglecting inertial term in momentum equation and assuming $\nabla\cdot\mathbf{J}=0$):

$$\frac{J_{\parallel in} - J_{\parallel is}}{B_i} = \frac{\hat{\mathbf{b}}\cdot\vec{\nabla}V\times\vec{\nabla}p}{B} \qquad V = \int \frac{ds}{B}$$

- Ohm's law for ionosphere:

Field-line-integrated current (includes both hemispheres) $\longrightarrow \mathbf{J}_h = \vec{\vec{\Sigma}}\cdot\left(-\vec{\nabla}\Phi\right)$

Field-line-integrated Conductivity (both hemispheres)

- Using conservation of ionospheric current: $\vec{\nabla}\cdot\vec{\mathbf{J}}_h = J_{\parallel}\ \sin(I)$
- And combing the above two gives "Fundamental equation of ionosphere-magnetosphere coupling":

$$\vec{\nabla}_i\cdot\left[\vec{\vec{\Sigma}}\cdot\left(-\vec{\nabla}_i\Phi\right)\right] = \hat{\mathbf{b}}\cdot\vec{\nabla}_i V\times\vec{\nabla}_i p\ \sin(I)$$

RCM Conceptual Diagram

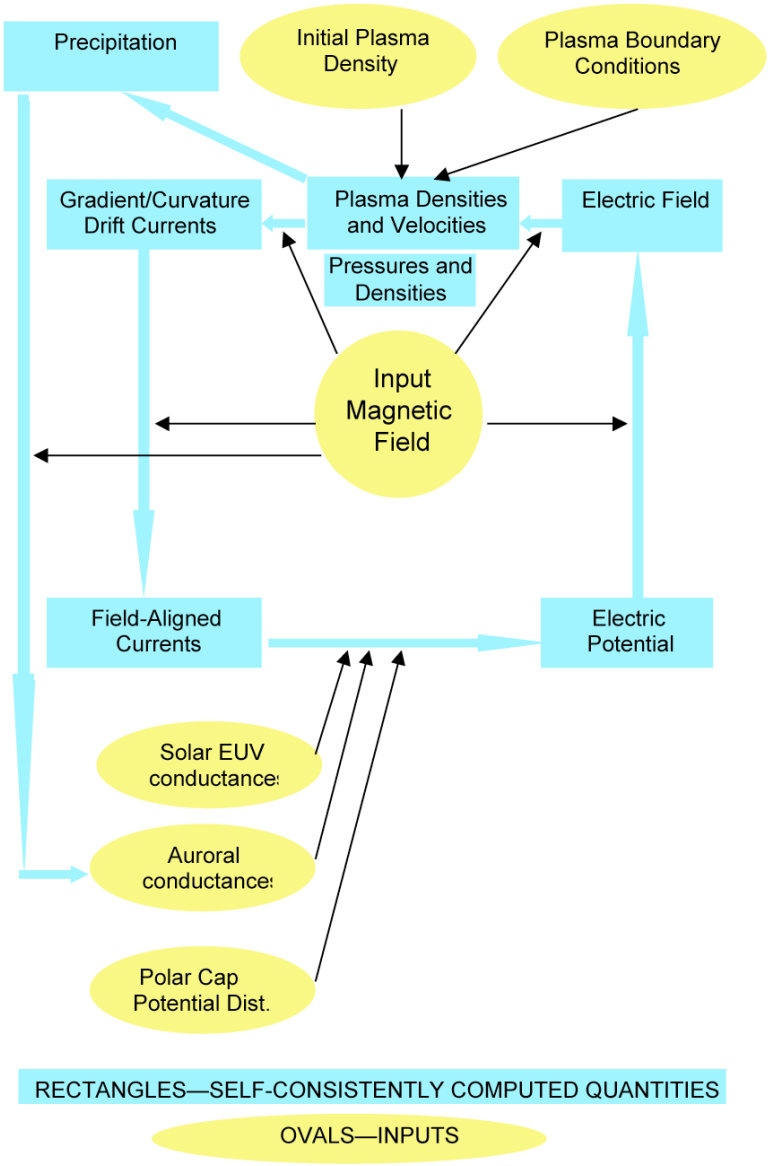

Basic RCM Physics

Alfven layer formation

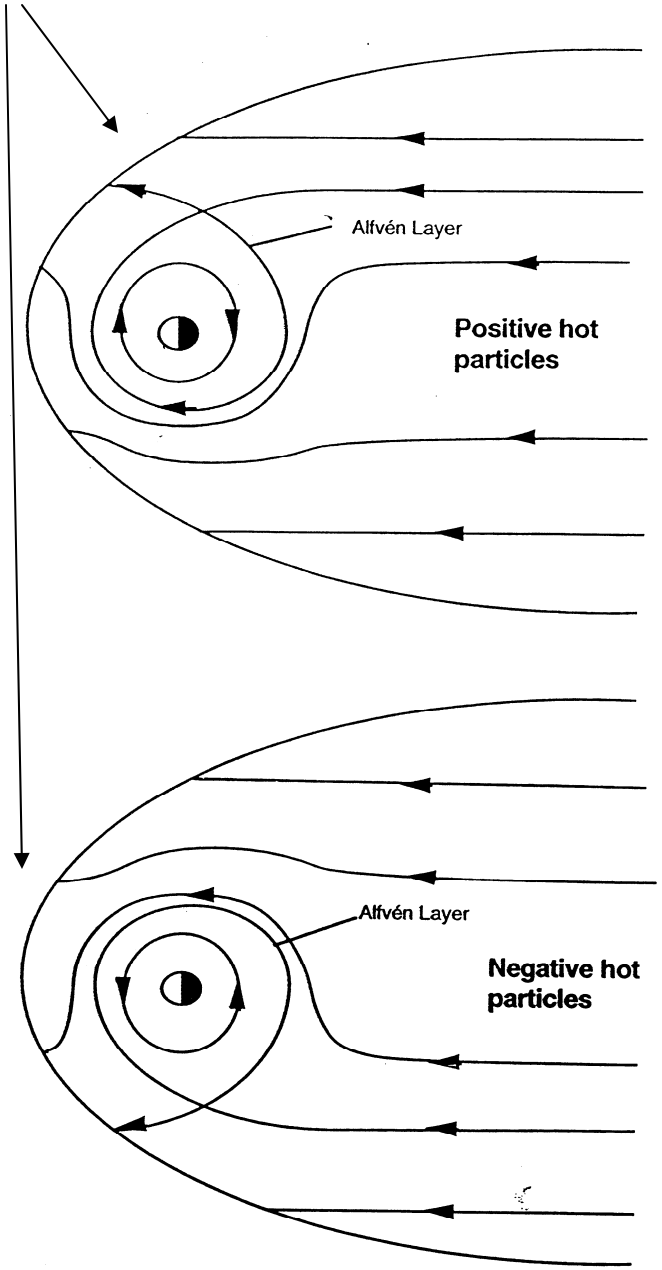

Inner magnetospheric electric field shielding

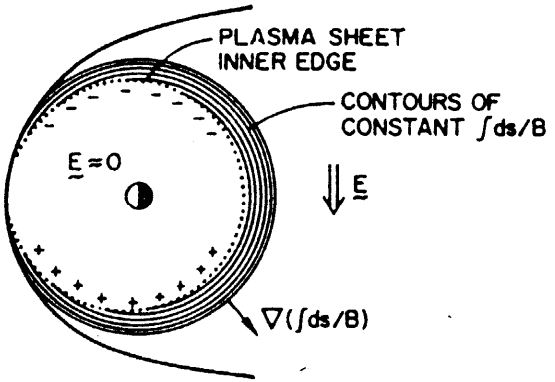

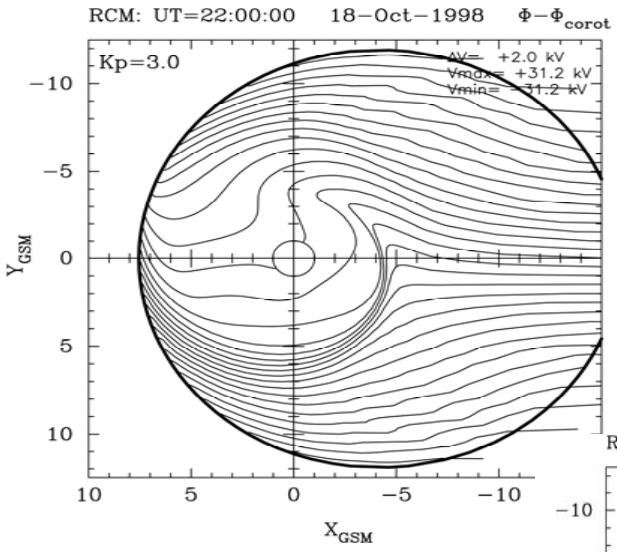

Formation of region-2 field-aligned currents

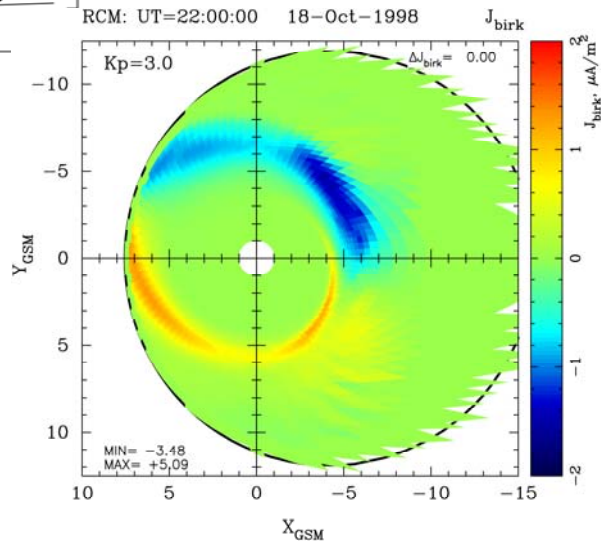

Standard Interpretation of Ring-Current Injection

- Standard Picture
  - Strong convection moves the Alfvén layer and plasma-sheet inner edge earthward.
  - Creates a partial ring current centered near midnight
  - Particles drift west, causing the center to move toward dusk.
  - If the convection remained strong, those injected ions would drift out of the magnetopause
  - If the convection weakens after > half a drift period, the Alfvén layer moves out, and some ions get trapped on closed drift shells.
- Direct injection of ions from the ionosphere onto inner-magnetospheric field lines also contribute to the ring current
  - Mostly at lower energies
  - We don’t have a theoretical estimate of how big the contribution is.

RCM with uniform dawn-to-dusk electric field

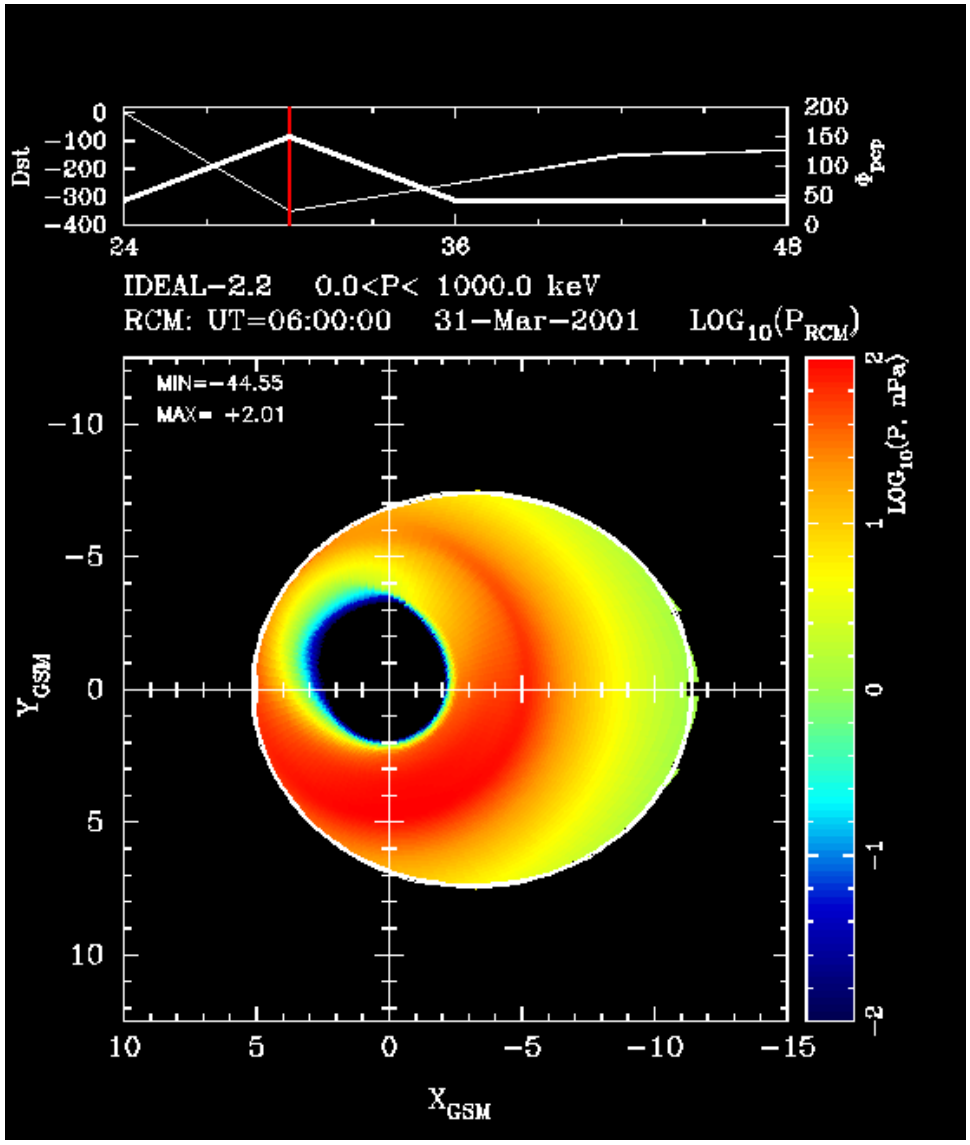

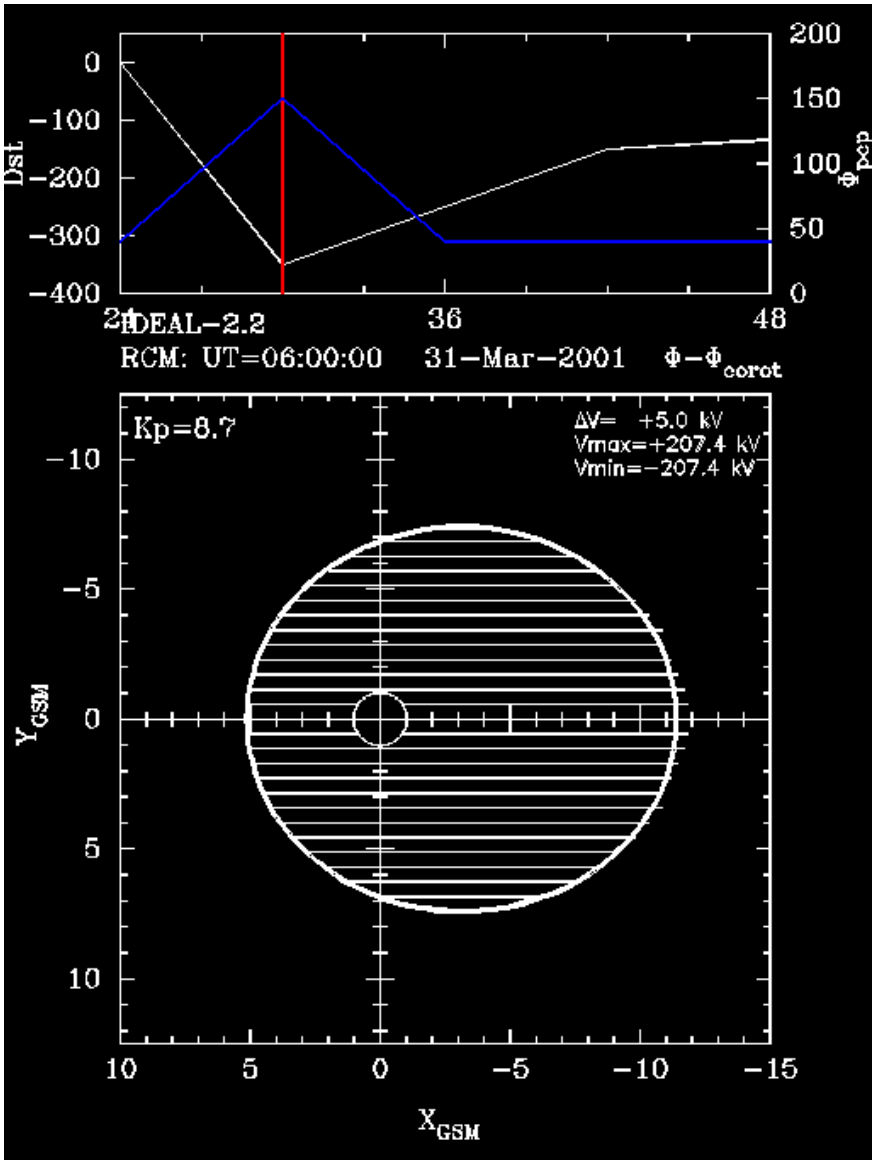

Full RCM

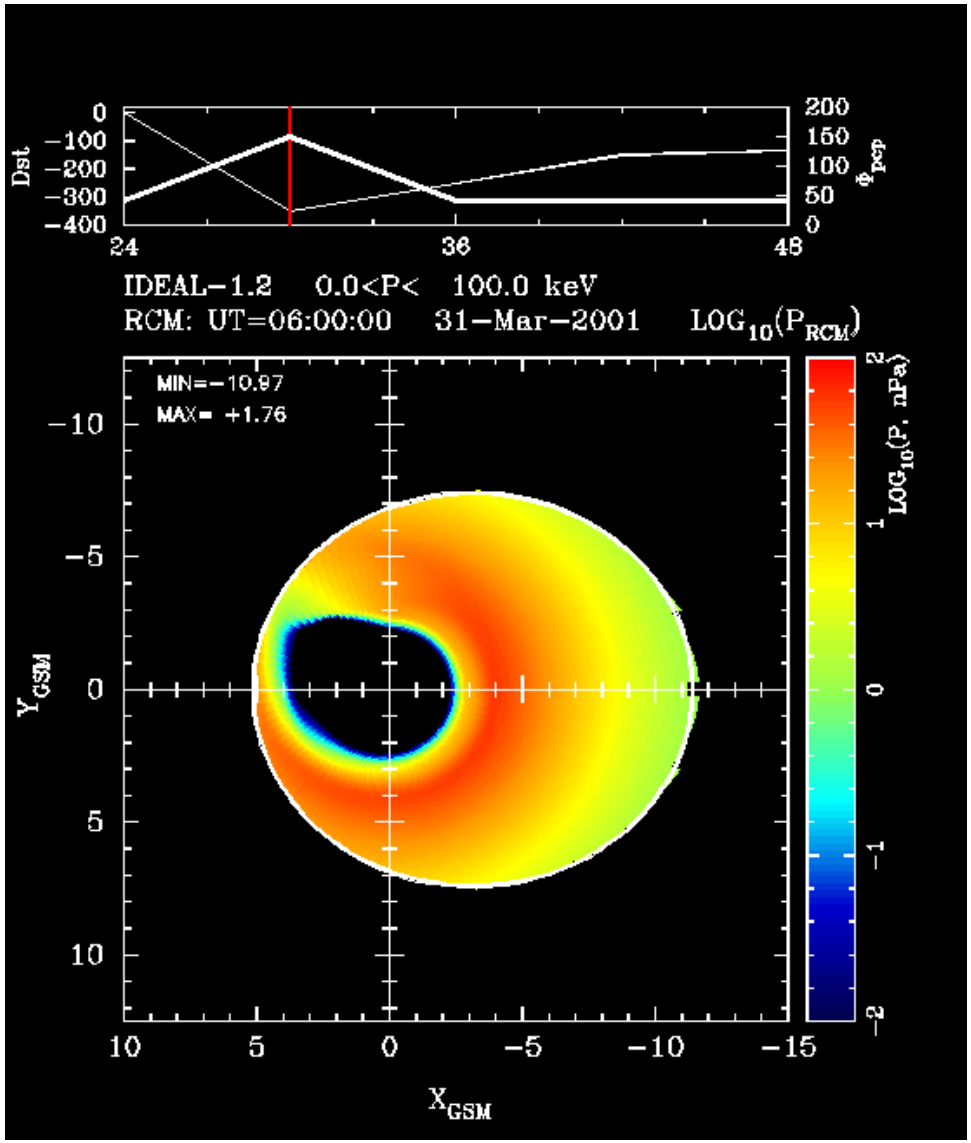
Dst
0
−100
−200
−300
−400
24
36
48
200
150
100
50
0
Φ_{pcp}
IDEAL−1.2 0.0<P< 100.0 keV
RCM: UT=06:00:00 31−Mar−2001 $LOG_{10}(P_{RCM})$
MIN=−10.97
MAX= +1.76
Y_{GSM}
X_{GSM}
$LOG_{10}(P, nPa)$

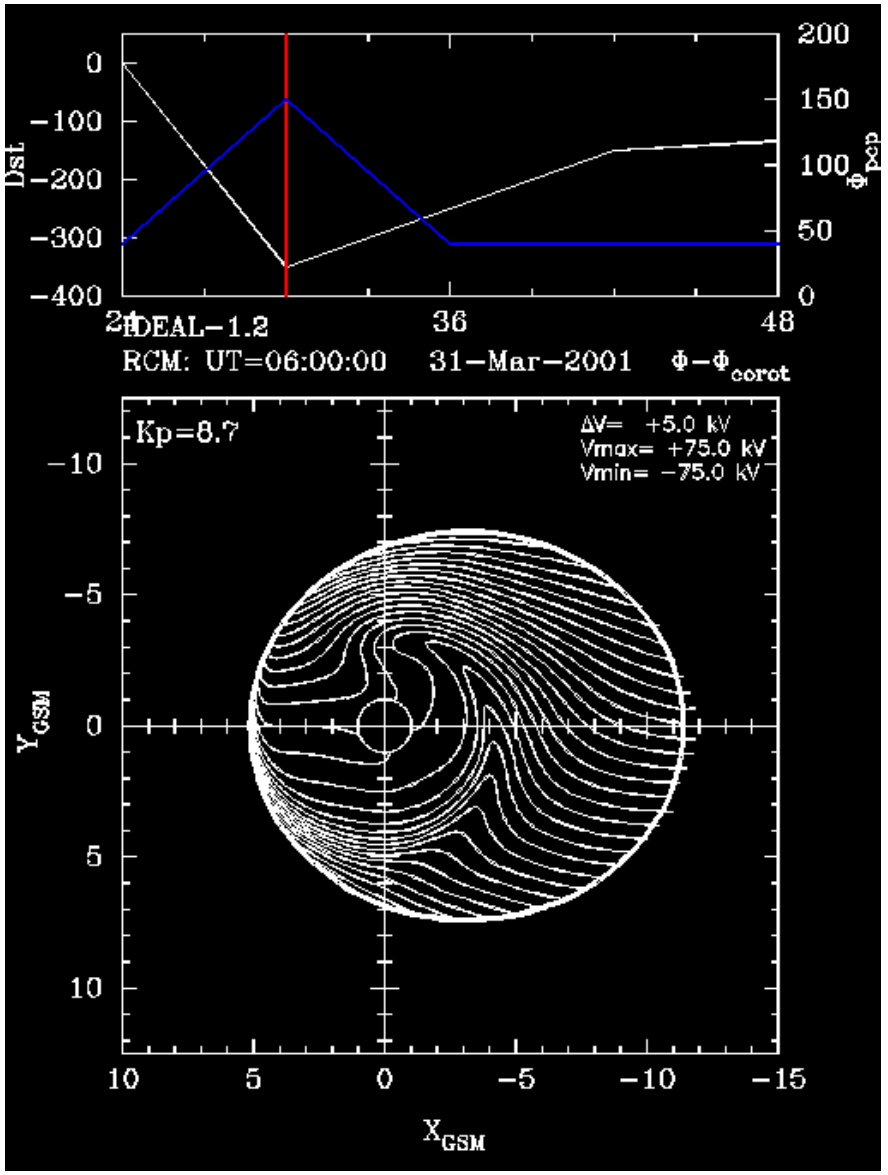
Dst
0
−100
−200
−300
−400
24
36
48
200
150
100
50
0
Φ_{pcp}
IDEAL−1.2
RCM: UT=06:00:00 31−Mar−2001 $\Phi-\Phi_{corot}$
Kp=8.7
ΔV= +5.0 kV
Vmax= +75.0 kV
Vmin= −75.0 kV
Y_{GSM}
X_{GSM}

Plasmapause simulation with the RCM

Hilmer-Voigt

T03

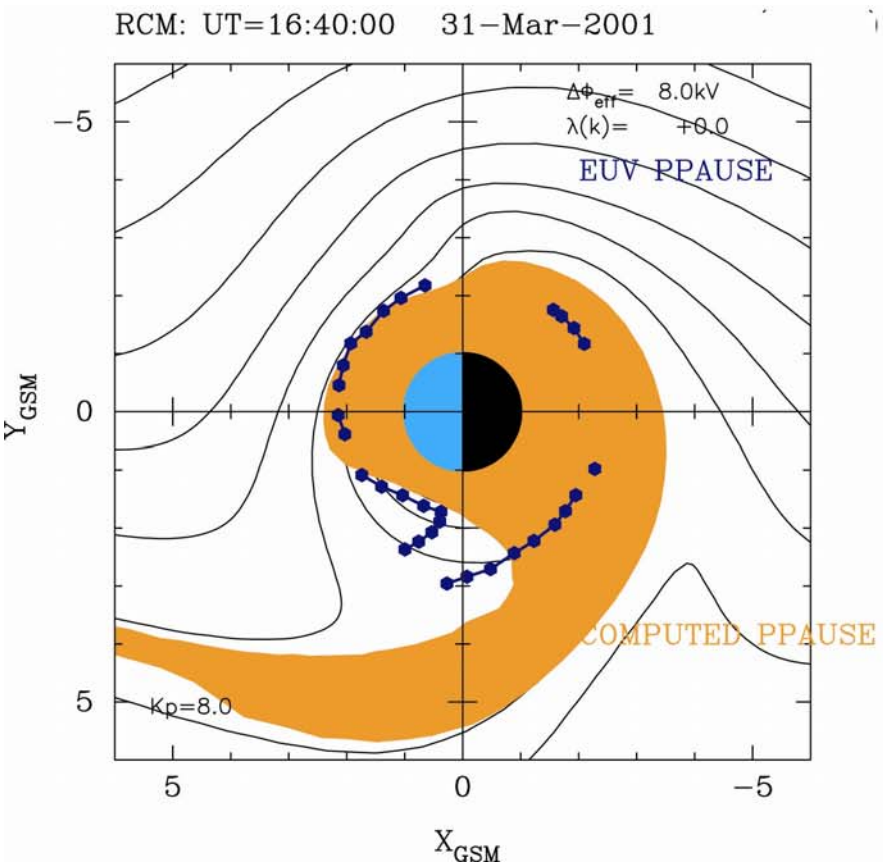

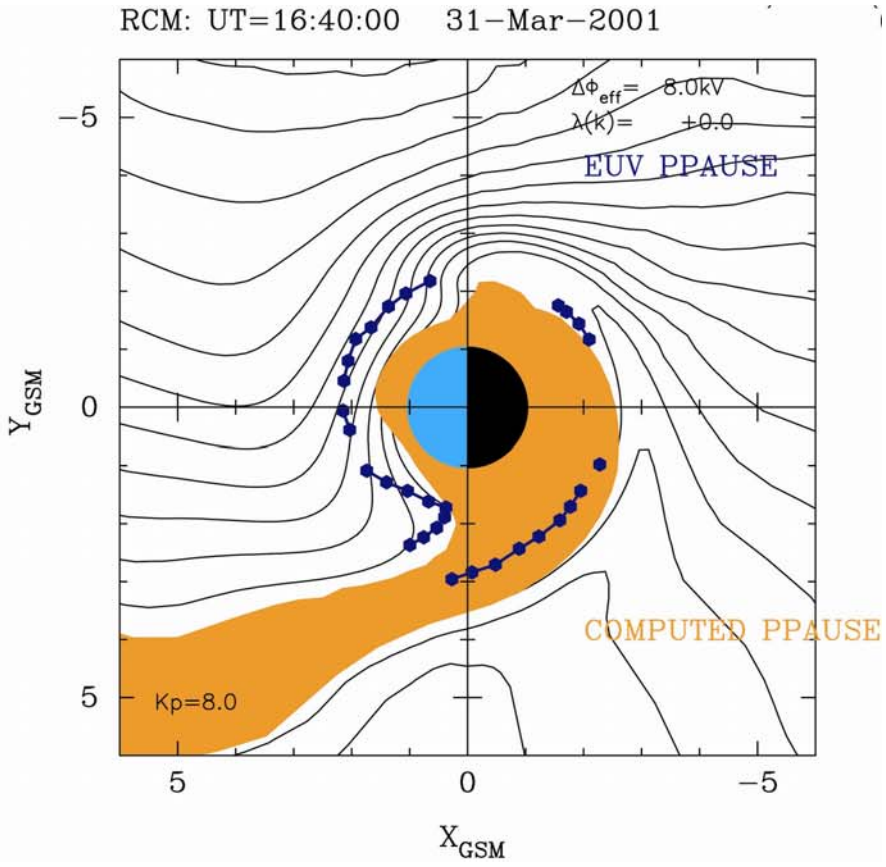

Plasmasphere is treated as a zero energy channel in the RCM.

IMAGE Observations of Ring Current Injection

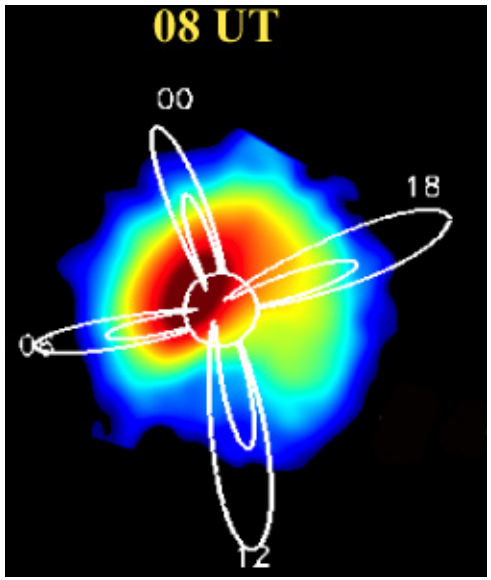

IMAGE ENA, 27-39 keV

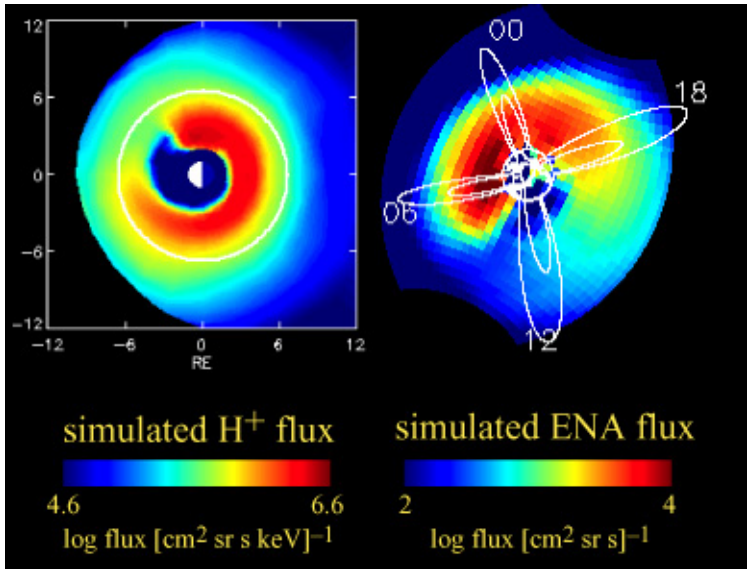

CRCM Model, 8 UT, 32 keV

- Observations and the CRCM model fluxes for 12 August 2000, at the peak of the main phase of a storm. Ring current peaks between midnight and dawn in both observation and model. From Fok et al. (submitted to *Space Sci. Rev.,* 2002)

Comments on Magnetic Storms

- Steady strong convection doesn't create a trapped ring current.
- Trapping fresh ring current particles requires a period of strong convection followed ~ half a drift period later by a period of weak convection.
- Note:
  - Westward-drifting tongue of particles
  - Successive periods of strong convection allows deeper injections of some particles.
- The biggest magnetic storms usually result from coronal mass ejections that create large plasmoids containing strong magnetic fields.
  - Strong southward IMF for half of the plasmoid.

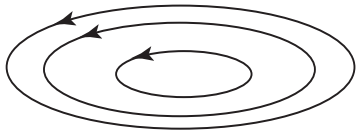

- We think we basically understand the injection of the storm-time ring current. The biggest remaining issue:
  - What is the relationship between substorms and storms?

The polarity of Bz in a magnetic cloud is solar cycle dependent

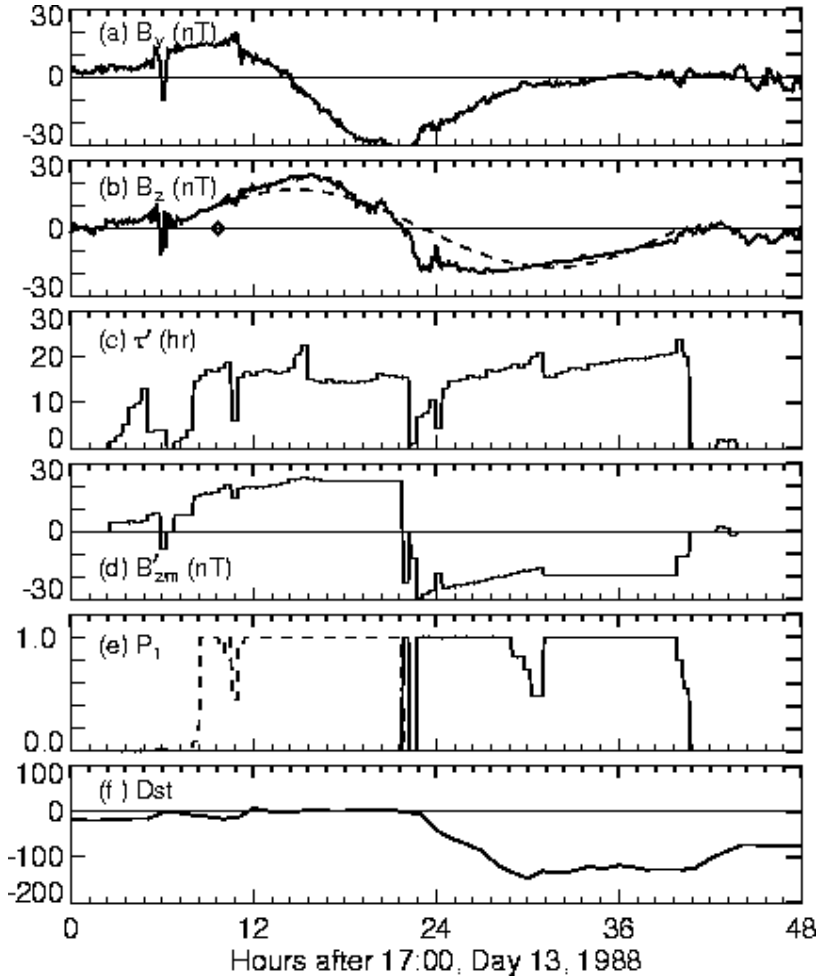

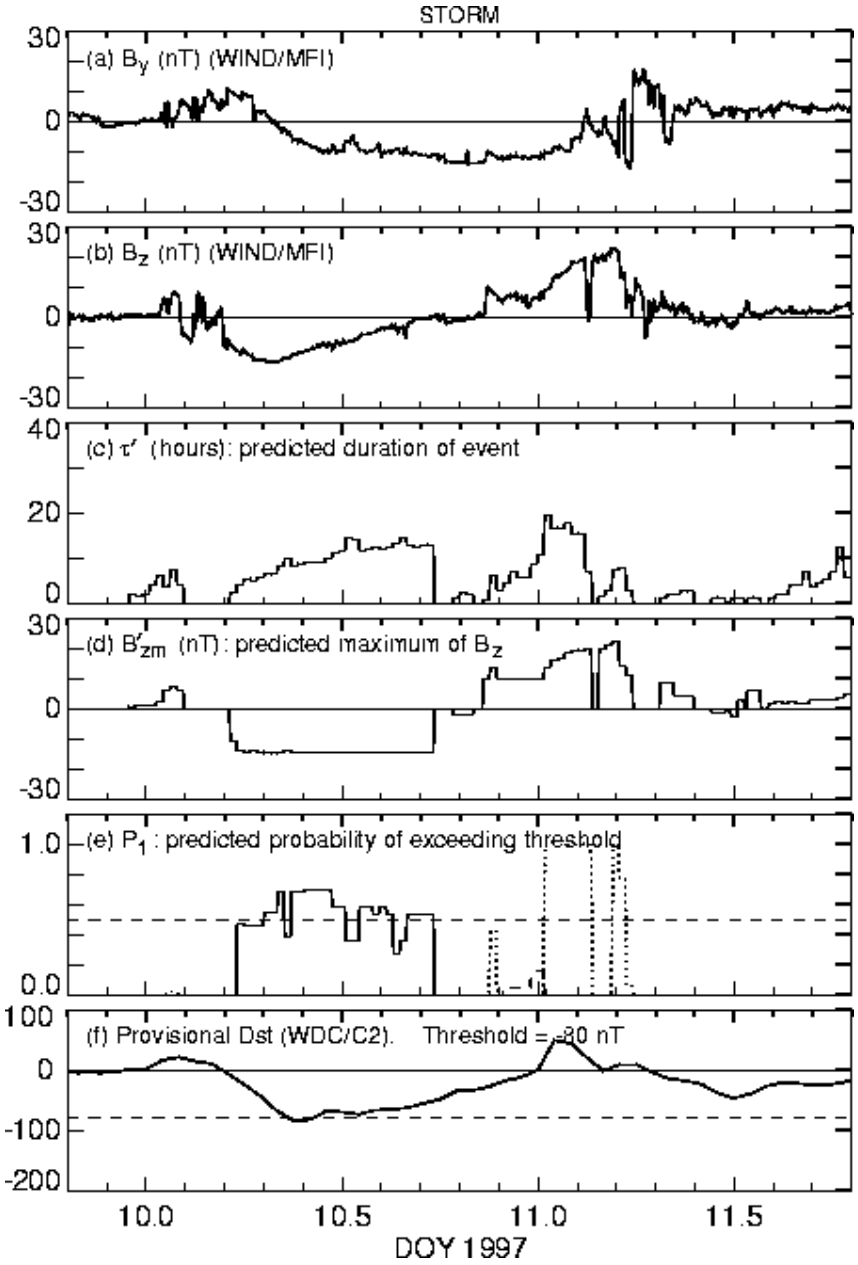

Comparison of Ring Current and Plasma-Sheet Energy Densities

- If the whole plasma sheet ion population was adiabatically convected from 15 R_E to 4 R_E, one would expect

$$\frac{u(4R_E)}{u(15R_E)} \sim \left(\frac{V(15R_E)}{V(4R_E)}\right)^{5/3} : (200)^{5/3} \sim 6800$$

- From data (Smith and Hoffman figure),

$$u(L=4)_{main\ \ phase} \approx 3\times10^{-7} erg/cm^3$$

$$u(15R_E) \sim (0.3cm^{-3})(8keV) \sim 4\times10^{-9}$$

$$\frac{u(L=4)}{u(15R_E)} \sim \frac{3\times10^{-7}}{4\times10^{-9}} = 75$$

- Most experts believe that the ring current ions come mostly from the plasma sheet.
- Part of the discrepancy between the "predicted" and observed ratios is due to the fact that the higher-energy part of the plasma-sheet ion distribution doesn't penetrate to *L*=4.
  - Convection isn't strong enough to do it.
- Part of the discrepancy remains unresolved and is controversial.

Effect of a self-consistent magnetic field

- Lemon et al, (GRL 2004) used the RCM-E where the input was a steady southward IMF
  - The RCM-E adjusts the magnetic field in order to maintain MHD equilibria with the RCM-computed pressures
  - The result of including a self-consistent magnetic field in the model was to inhibit ring current formation

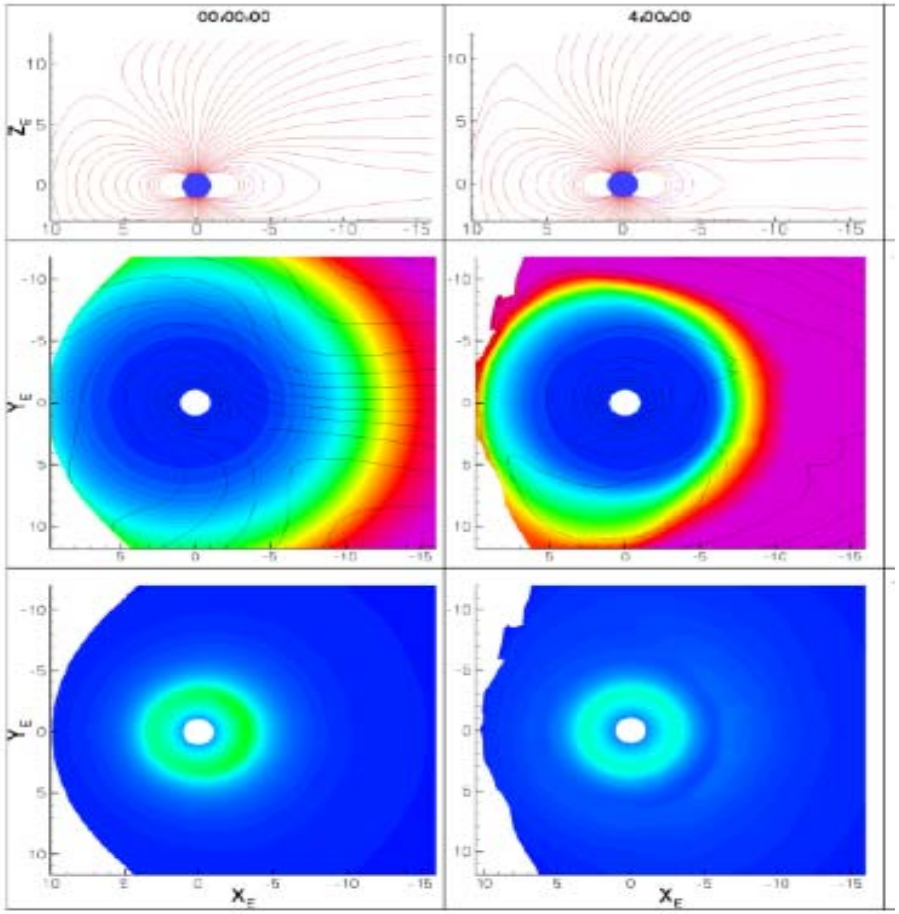

Magnetospheric Substorms

The Substorm

- Despite over 25 years of research, the magnetospheric substorm is arguably the most basic unsolved problem in magnetospheric physics.
  - It is a source of embarrassment in magnetospheric physics.
  - Sessions at meetings, such as at AGU, are typically full of contentious and often bitter arguments between rival factions.
  - The arguments typically boil down to explaining what is the actual sequence of events during a substorm.
  - The sparsity of data added to the overall confusion about the subject especially in the ambiguity of determining when and where a substorm starts.
- The recent launch of the multi-satellite THEMIS mission that was specifically designed to look at substorm, has the potential to make significant advances towards solving the problem, or it may simply add to the complexity of the problem.
  - THEMIS has a significant ground-based component.

Auroral Substorm: Akasofu Picture

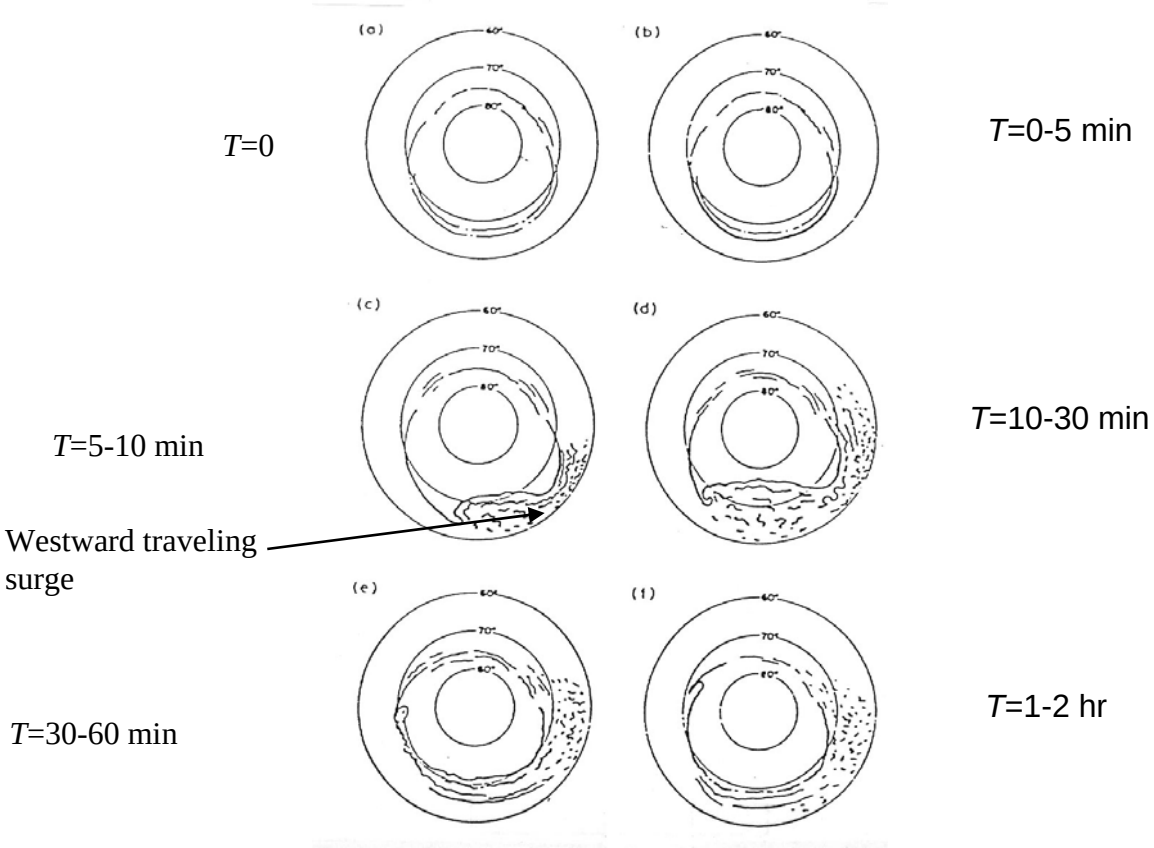

Figure from Akasofu (Polar and Magnetospheric Substorms, D. Reidel, 1968), summarizing ground observations of discrete aurora.

- This figure, from Akasofu's 1968 book, is one of the most famous in space physics.
- After more than 20 years of satellite photos of aurora, Akasofu's summary is still accepted.

Polar VIS Image of Substorm

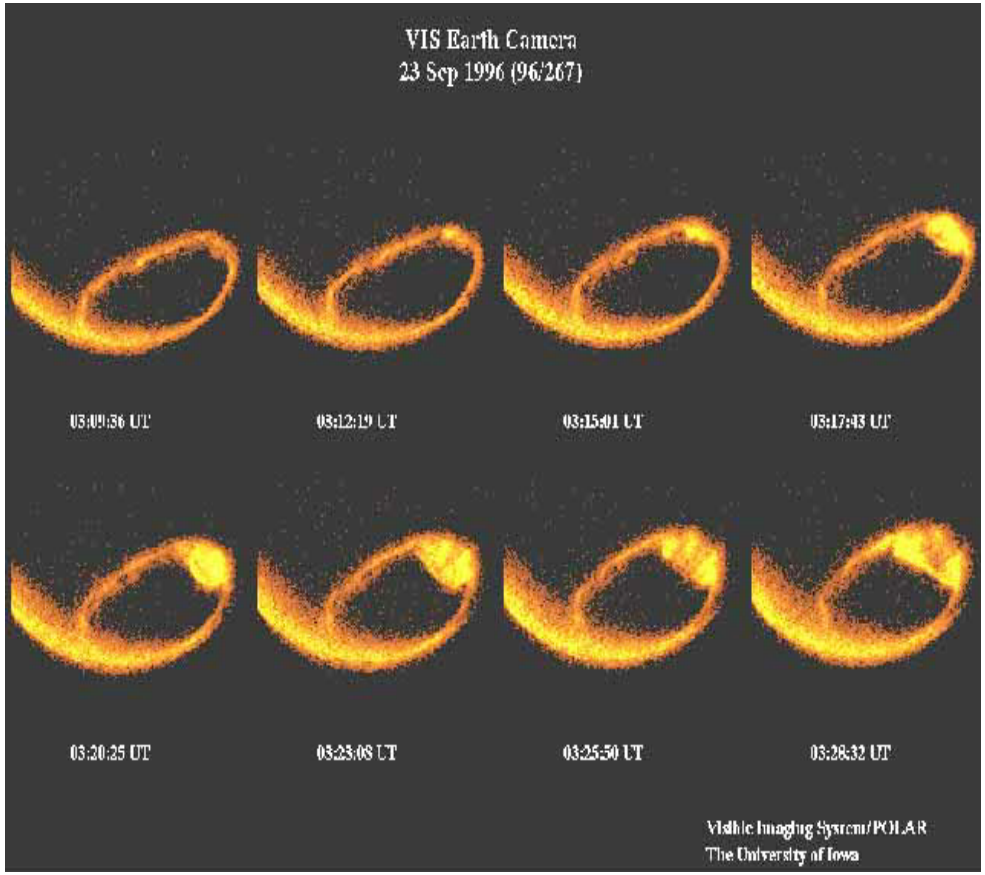

The Solar-Wind in a Substorm

Solar Wind Driver

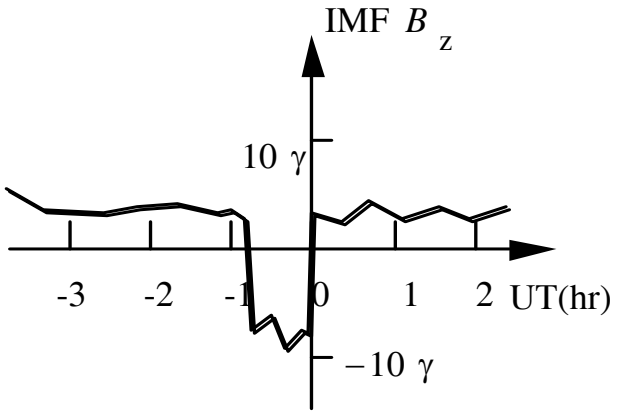

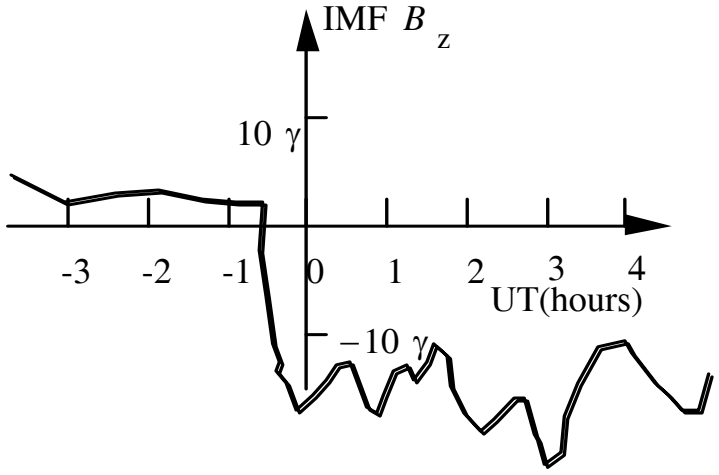

Magnetospheric Result

Isolated substorm:

Growth phase starts about - 0.75 hr
Expansion phase onset about 0 hr
Short expansion phase followed by recovery to original condition

Magnetic Storm:

Well-defined substorm growth phase starts about - 0.5 hr. Onset of expansion phase about 0 hr. No clear recovery from first substorm. Lengthy period of substorm-like activity results in formation of ring current.

Substorm Phases

- The MAGNETOSPHERIC SUBSTORM involves a sudden, almost explosive release of energy.
- The substorm sequence is described in a series of phases
  - GROWTH PHASE
  - EXPANSION PHASE
  - RECOVERY PHASE
- However the substorm sequence is typically complex and poorly differentiated

Substorm Phases

- During the GROWTH PHASE of the classical substorm, the tail magnetic-field configuration gets very stretched, and the peak current density in the cross-tail current becomes very large.
  - Energy seems to be stored in the tail during the growth phase.
- An energy release begins suddenly at the onset of the EXPANSION PHASE. Field lines near local midnight, which had been very stretched and tail-like at the end of the growth phase, collapse to a more dipolar shape.
  - The aurora suddenly brighten, and the ionospheric conduction currents -- particularly the westward electrojet -- intensify greatly, usually in a limited region of the auroral zone near local midnight.
  - As the expansion phase proceeds, the region of dipolarization, bright aurora and intense currents expands.
  - A large substorm eventually affects nearly all of the nightside auroral zone.
- In the RECOVERY PHASE, the intense ionospheric currents and auroral activity gradually die out.
  - The post-substorm plasma sheet is hotter than it was before the substorm. One or more large substorms normally occur in the main phase of a magnetic storm.

Changes in Inner Plasma Sheet

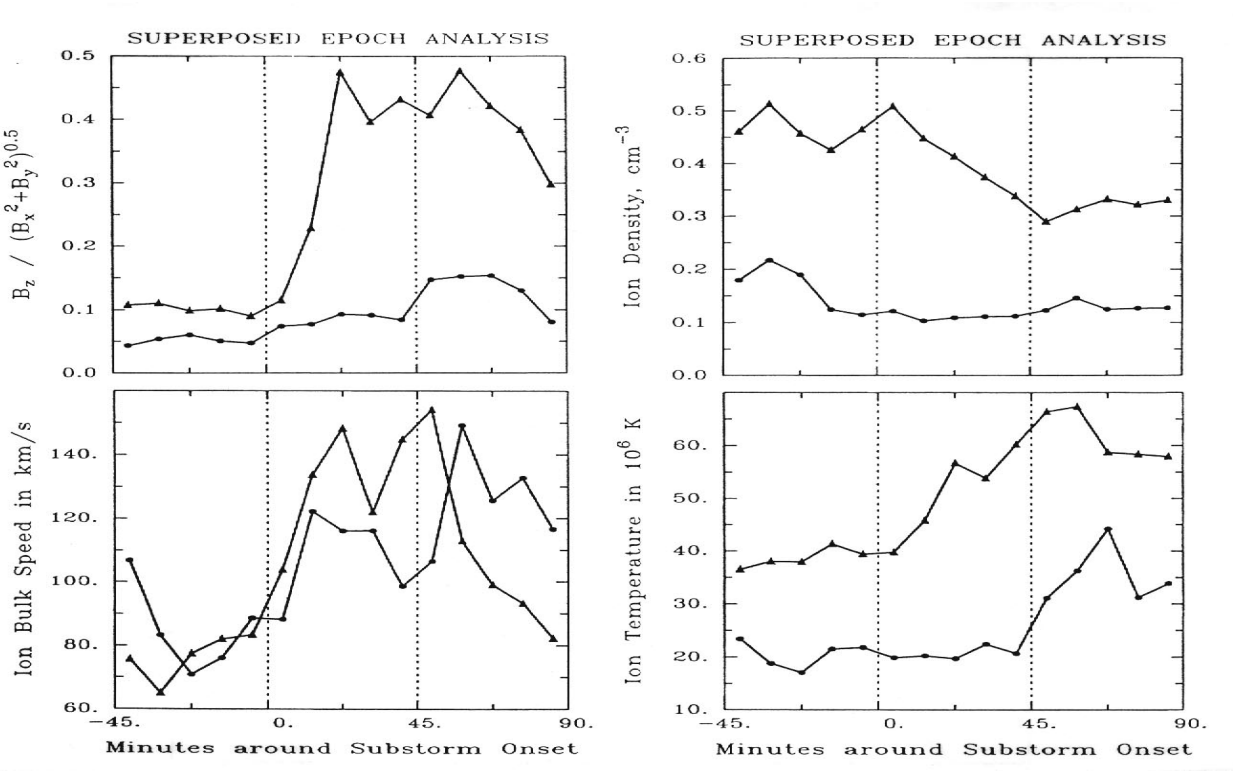

- Superposed epoch analysis for inner plasma sheet out to 18 R_E.
- Note that field becomes dipolar.
- Flow speed becomes earthward.
- Ion temperature increases in expansion phase.

Geosynchronous Orbit Particles–Growth Phase

- C2 index is the coefficient of the $P_2(\cos\alpha)$ in a fit to the angular distribution of 40 keV electrons. C2 > 0 implies a cigar shaped distribution, with more flux along **B** than perpendicular to it.

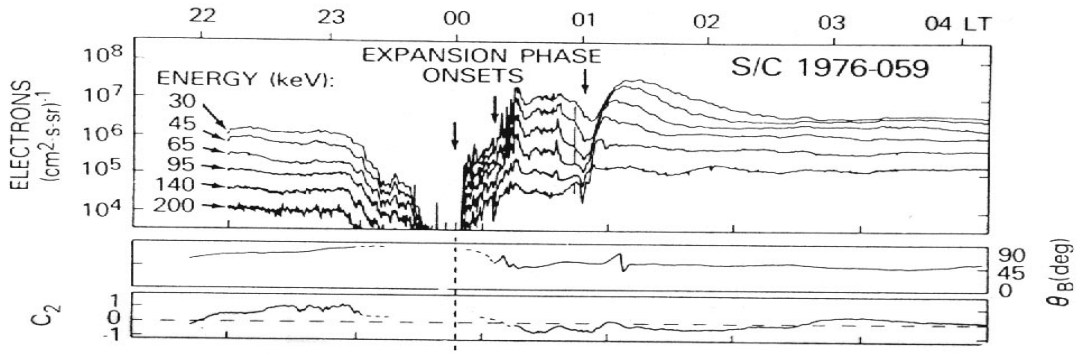

- Note that the pitch-angle distribution becomes cigar shaped in the growth phase as the growth-phase develops.
- Then the geosynchronous flux drops out.

Substorm Currents and Magnetic Field Changes–Midlatitude Magnetogram

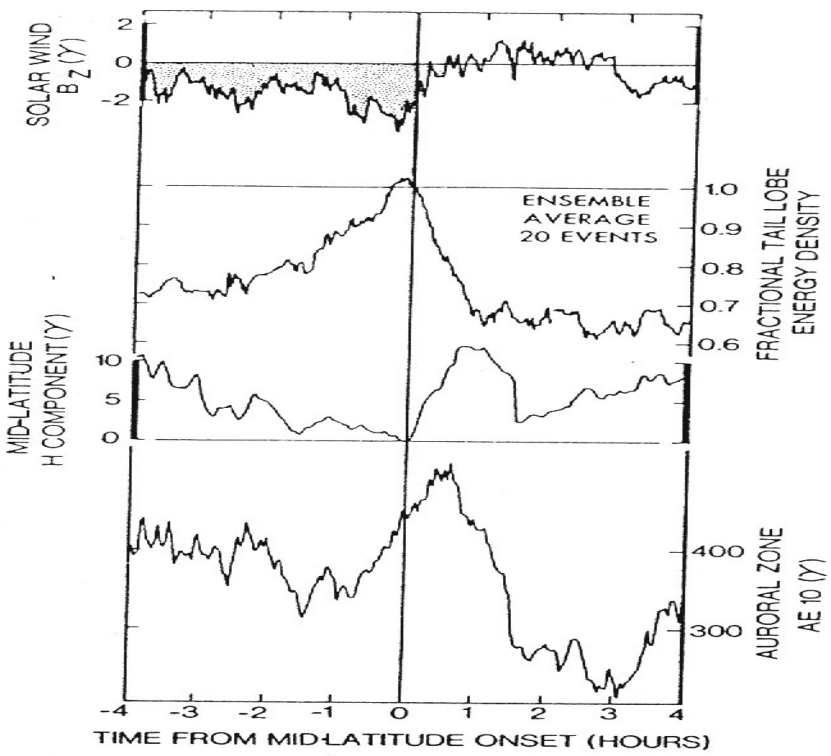

Superposed epoch averages of IMF B_z, tail-lobe magnetic energy density, midlatitude magnetic perturbation near center of substorm, and AE. From Caan et al. *(JGR*, *80*, 191, 1975).

- IMF B_z tends to be negative before onset, slightly northward after.
- Tail lobe magnetic energy increases during growth phase, decreases in expansion phase.
- Note strengthening of horizontal field at midlatitude, near center of substorm sector.

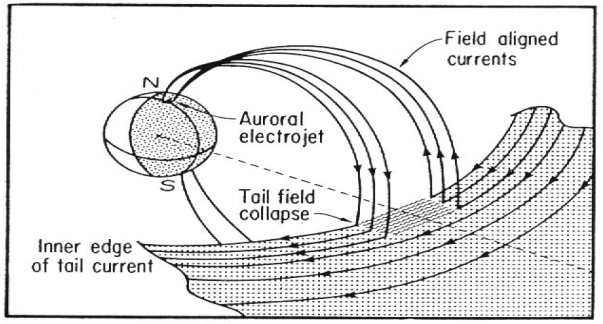

Interpretation in terms of substorm current wedge

High-Latitude Substorm Currents

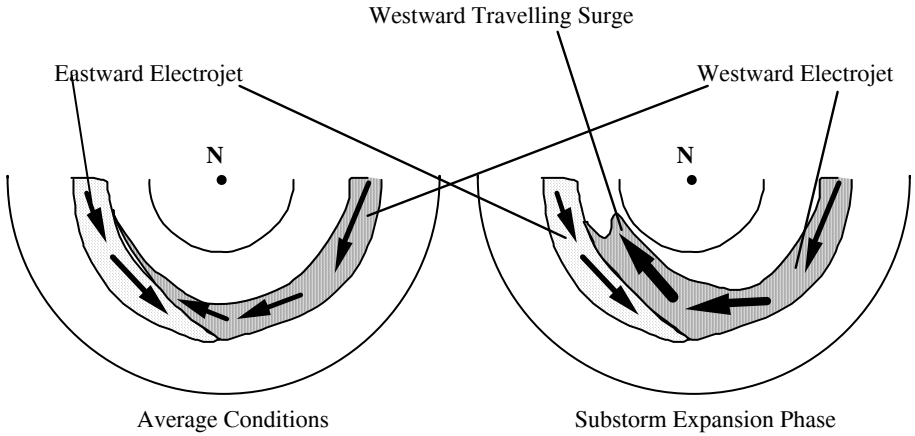

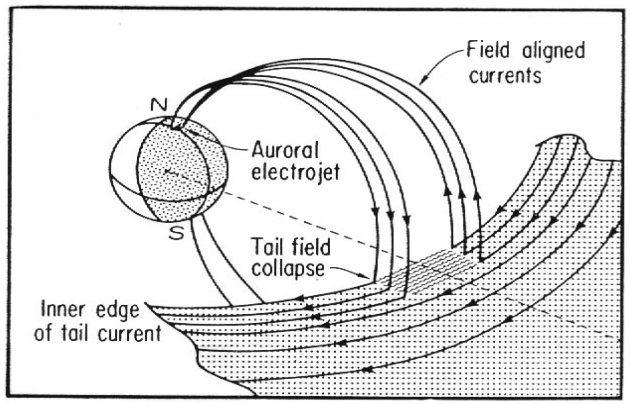

From McPherron et al., *JGR*, *78*, 3131, 1973)

- Enhanced westward electrojet interpreted as ionospheric part of substorm current wedge.
- AE index is used to indicate the strength of the electrojet - measure from high latitude stations.

Changes in Middle Plasma Sheet (~ 30 R_E)

- From Geotail spacecraft, which spent a long time with apogee ~ 30 R_E:
- Flow becomes antisunward in the center of the substorm.
- B_z typically switches from sunward to antisunward.

Midnight Region Near 8 R_E

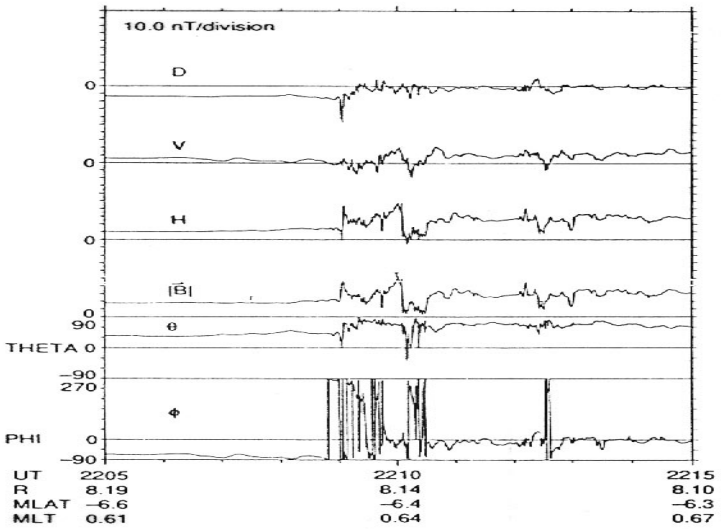

AMPTE-CCE magnetic fields (from Lopez et al., in *Magnetospheric Substorms*, *Geophys. Mono. 64*, 1991)

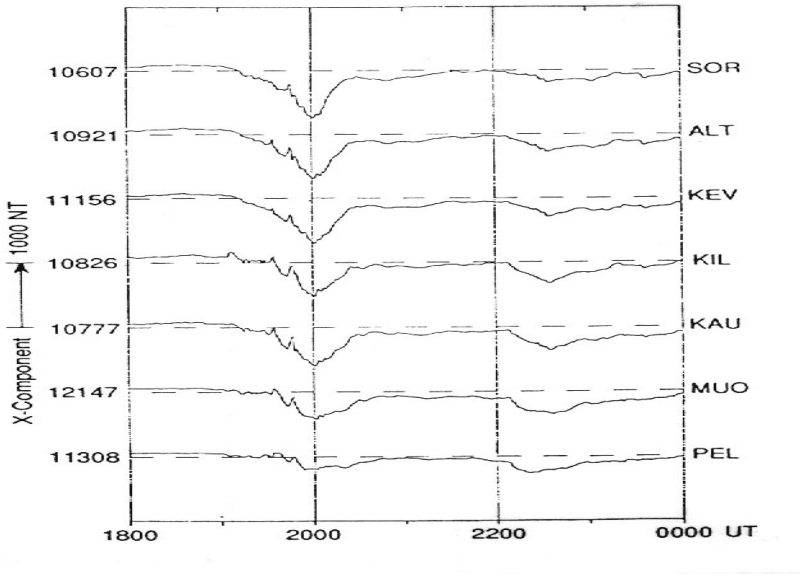

Ground magnetograms, northward component, from a chain of stations

- Note wild fluctuations in magnetic field near 8 R_E approximately coincident with beginning of ground magnetic disturbance.

Geosynchronous Particles in Expansion Phase

- In the 1970's Carl McIlwain started displaying data from geosynchronous spacecraft in terms of "spectrograms
- Elegant patterns appeared for nearly every substorm expansion phase.
- Each substorm injects fresh particles into the geosynchronous orbit region.
- McIlwain characterized the particles as originating just outside an "injection boundary," which originally was of a somewhat mystical nature.
  - The modern view is that the injection boundary is the inner edge of the plasma sheet, just after that region collapsed to dipolar form in the expansion phase.

Substorm Viewed by Meridian Scanning Photometers

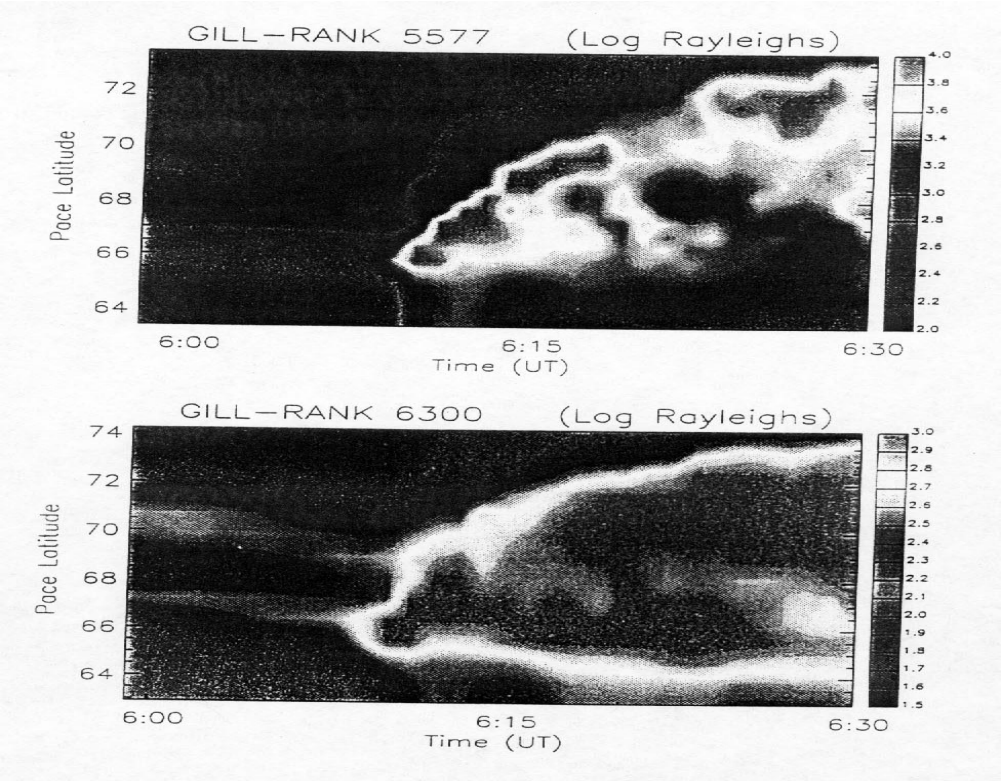

- Note that initial brightening is at about 66˚ latitude

$$L = \frac{1}{\cos^2 66^\circ} \approx 6$$

- Substorm X-line is typically observed at 25-30 R_E.

Near-Earth-Neutral-Line Model

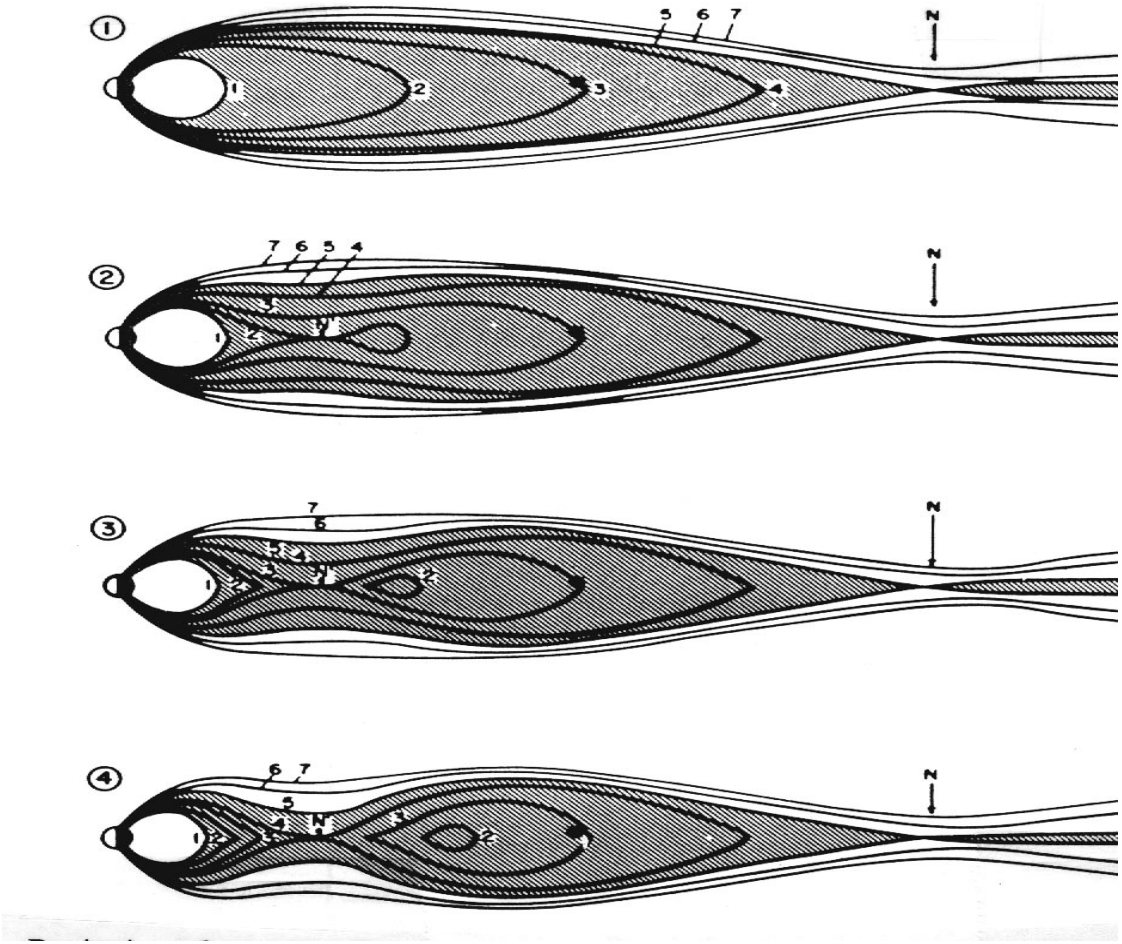

Growth phase

X-line forms in middle plasma sheet

Reconnection proceeds and plasmoid grows

NENL model, from Hones (*JGR*, *92*, 5633, 1977)

Near-Earth-Neutral-Line Model

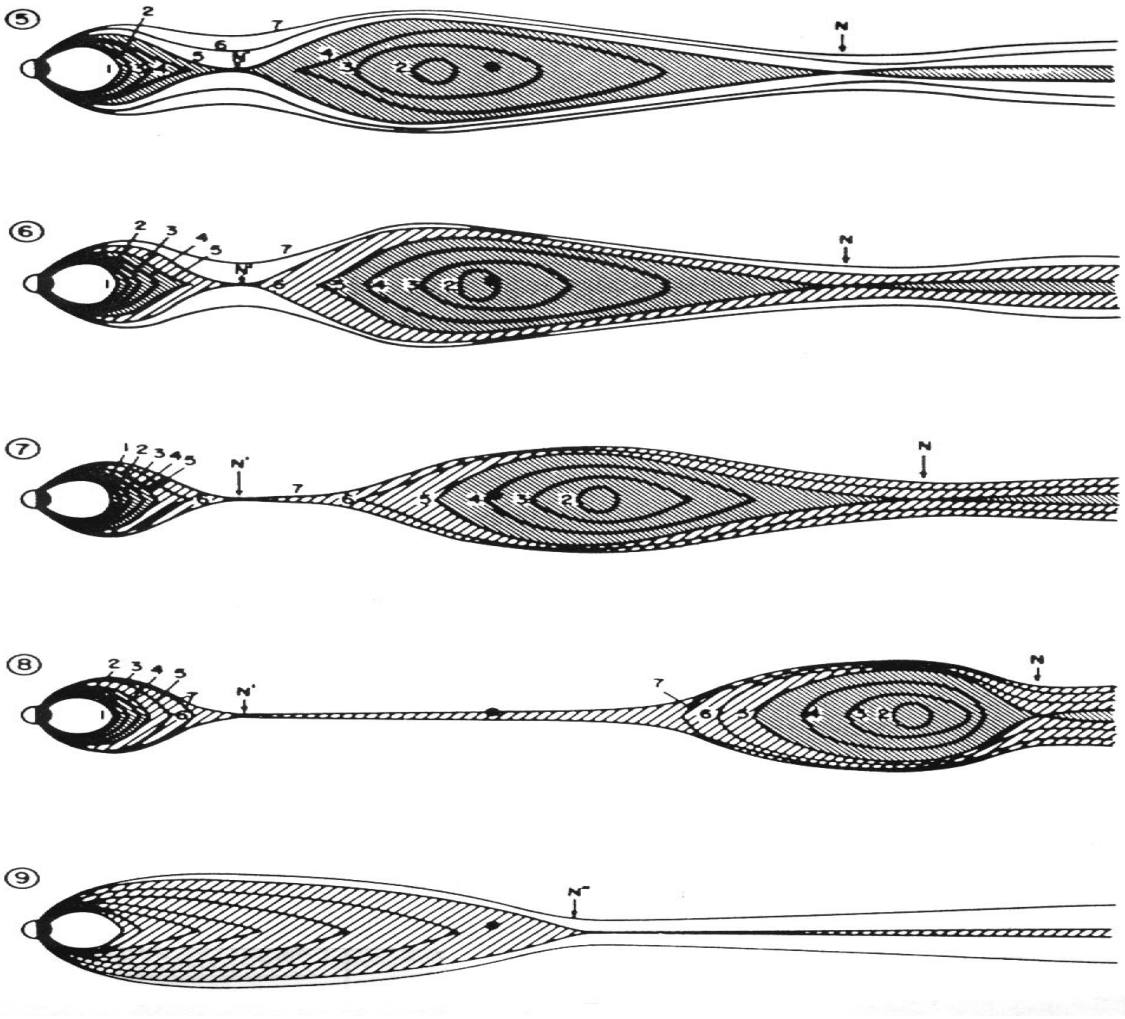

X-line eats it way through all closed field lines

Plasmoid moves antisunward

Recovery phase: Plasma sheet refills

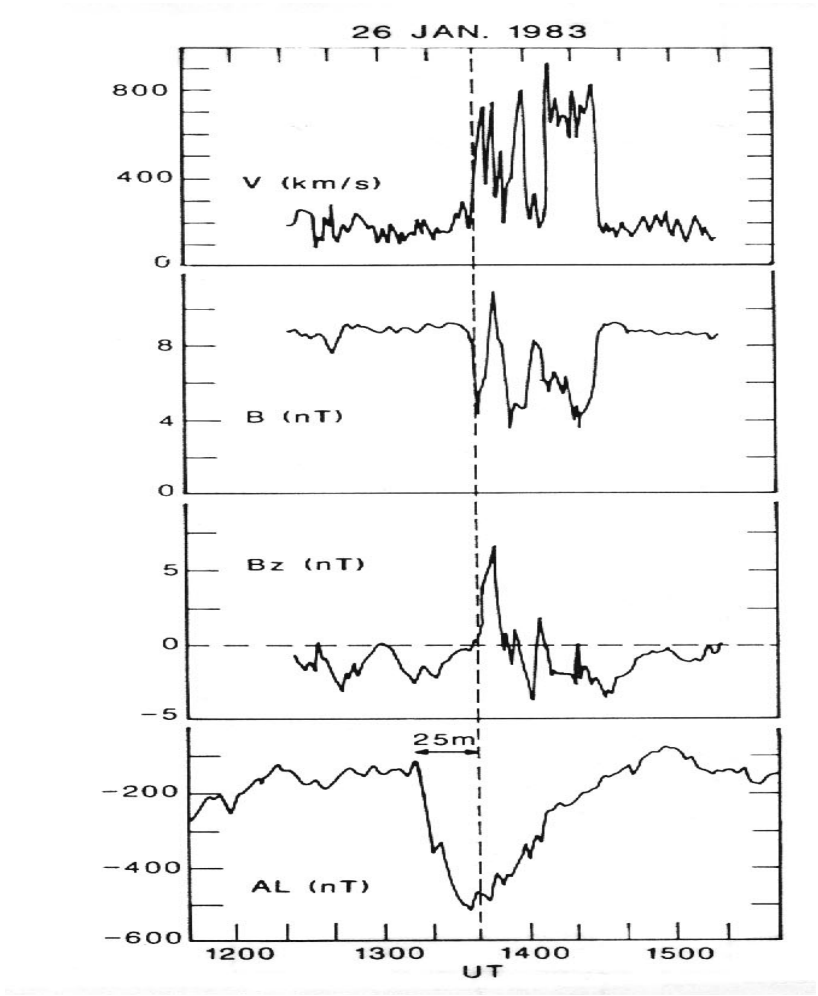

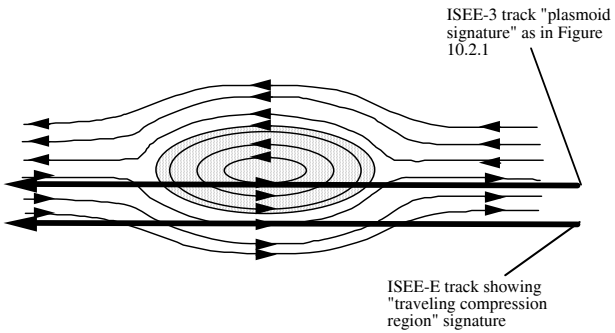

Distant Tail in a Substorm

- Flow velocity *V*, field magnitude *B*, northward component B_z, from ISEE 3 spacecraft.
- The high-flow event is interpreted as a plasmoid, with opposite signs of B_z.
- Note that plasmoid arrives shortly after the time of strongest electrojet.

(From Baker et al., in Magnetotail Physics, ed. A. T. Y. Lui, 1987)

Reconnection in Solar Corona and Geotail

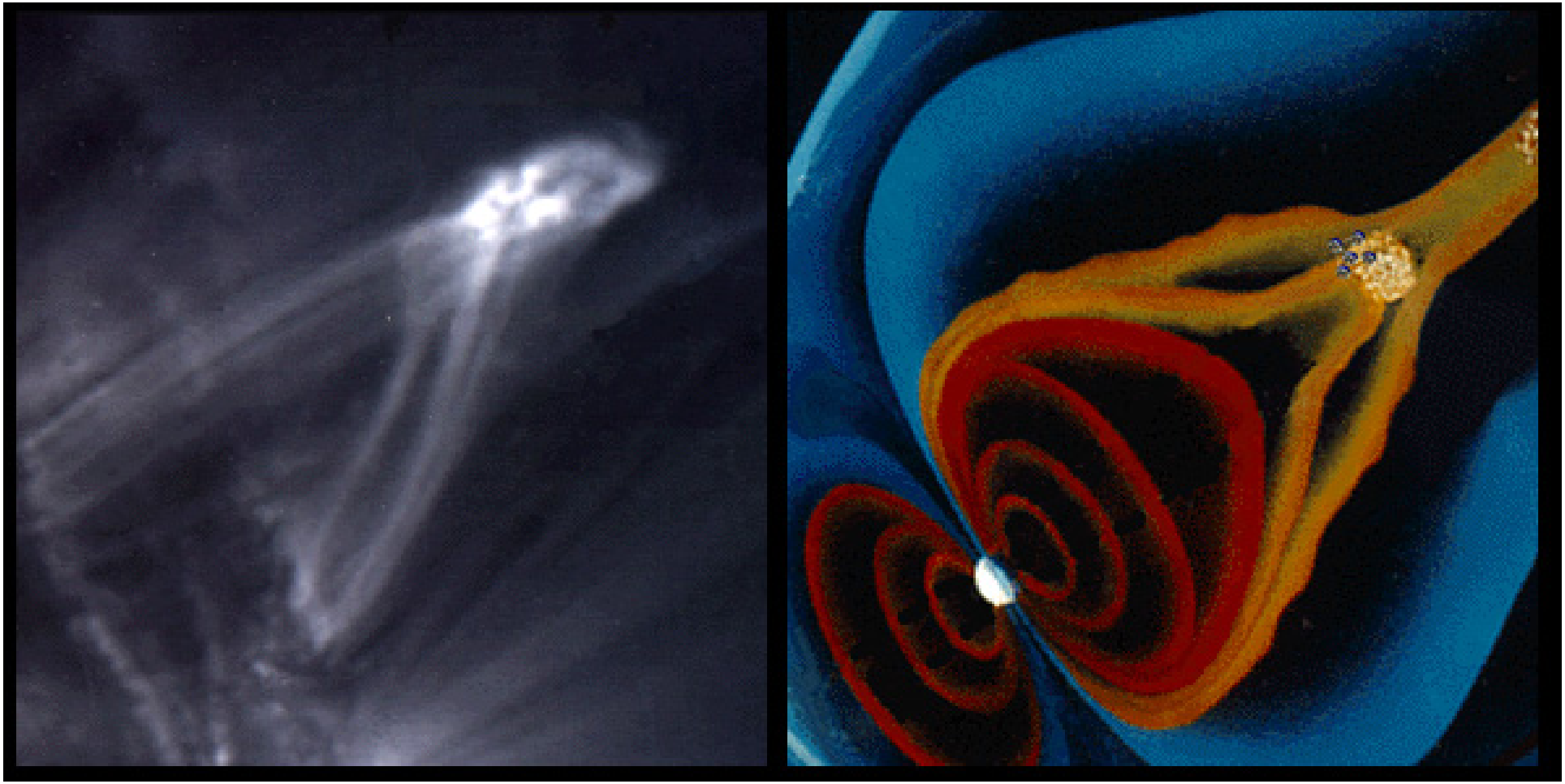

Same absolute scale in both pictures

Siscoe, 2004

Melon-Seed Magnetic Geometry

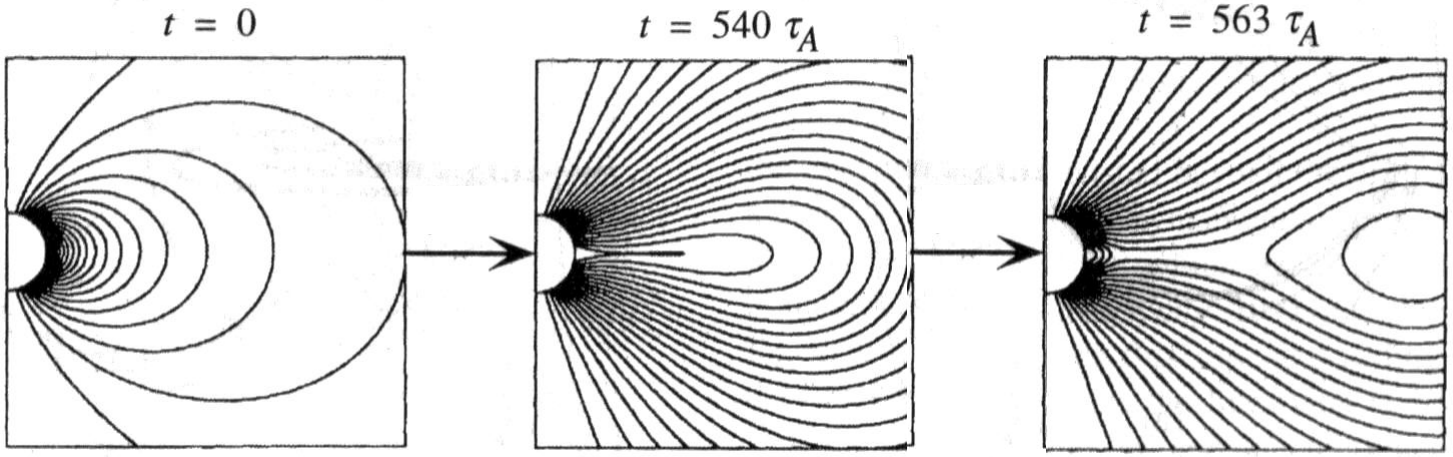

Mikic and Linker

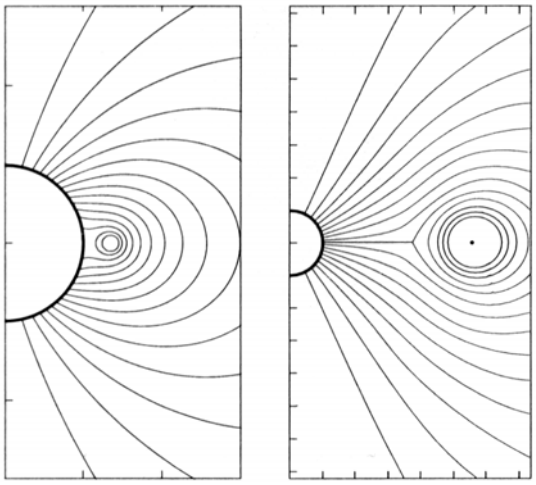

Forbes

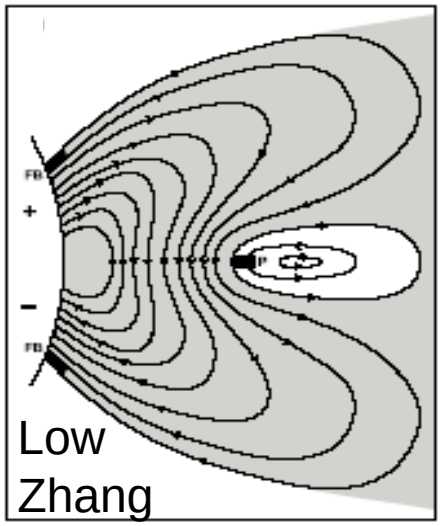

Low
Zhang

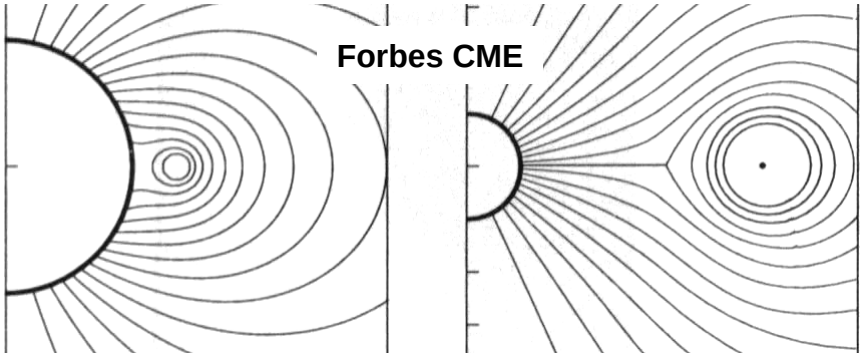
Forbes CME
Hones TPE

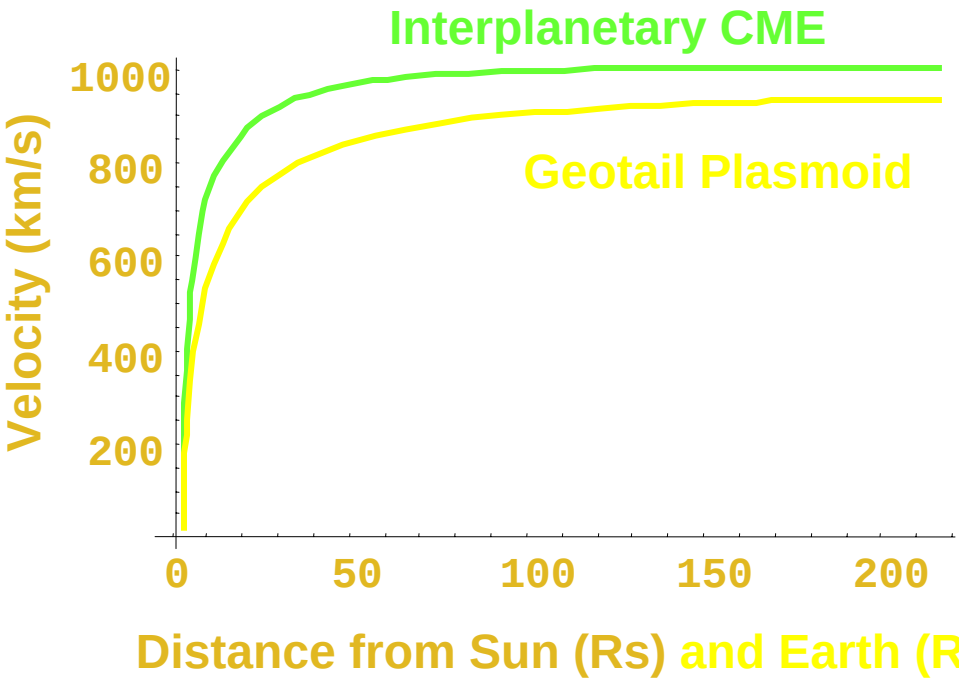
Interplanetary CME
Geotail Plasmoid
Velocity (km/s)
1000
800
600
400
200
0
50
100
150
200
Distance from Sun (Rs) and Earth (Re)

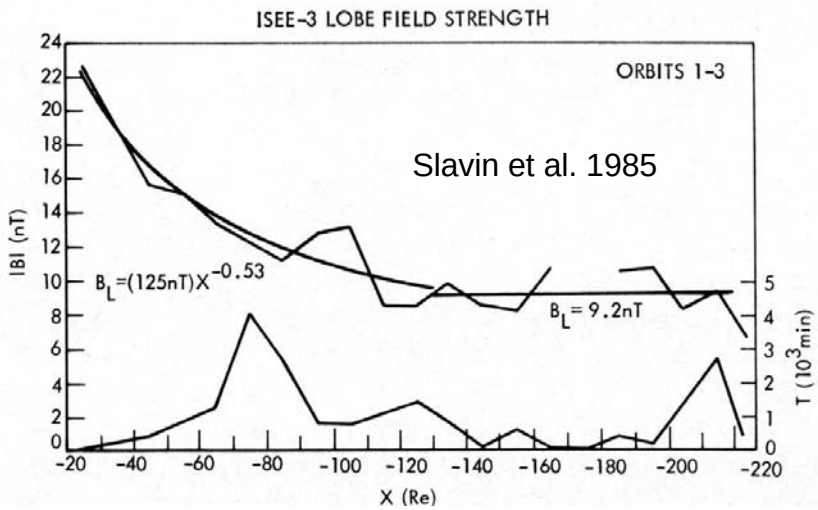
ISEE-3 LOBE FIELD STRENGTH
ORBITS 1-3
Slavin et al. 1985
|B| (nT)
$B_L=(125nT)X^{-0.53}$
$B_L=9.2nT$
T (10^3min)
X (Re)

Global MHD Simulation Illustrating Near-Earth Neutral

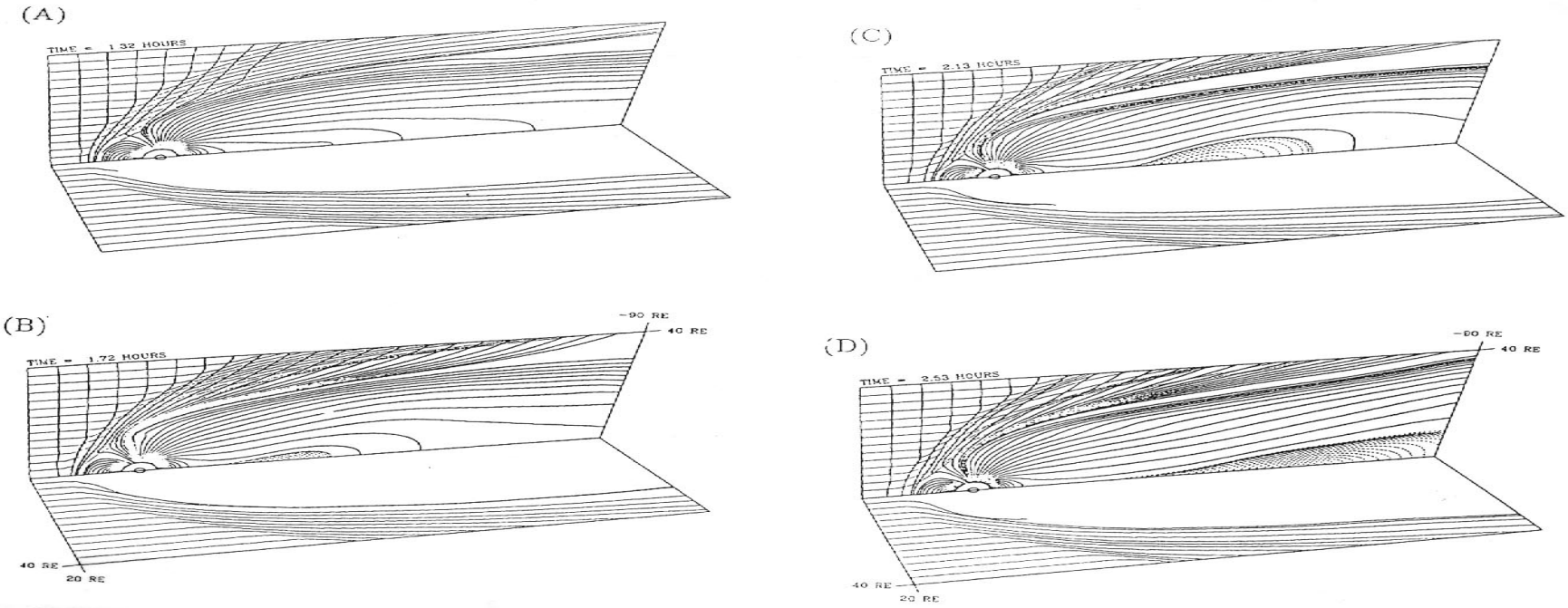

Formation of plasmoid in 3D global MHD simulation, for the case of a southward IMF. Configurations are shown at 1.5 hr. From Usadi et al. (*JGR*, *98*, 7503, 1993).

Advantages of the Near-Earth-Neutral-Line Model

- Geotail convincingly observed reconnection occurring at ~ 25 RE in substorm expansion phases.
- It predicted the tailward-moving plasmoids, years before they were observed.
- It has seen extensive theoretical development.
- Near-Earth neutral lines nearly always form in global MHD simulations for conditions of southward IMF.

Advantages of the Near-Earth-Neutral-Line Model

- It offers a natural interpretation of the substorm currents wedge, in terms of Vasyliunas' equation

$$\frac{J_{\|in}}{B_{in}} - \frac{J_{\|is}}{B_{is}} = \frac{\hat{\mathbf{b}}_{in}}{B_{in} V^{5/3}} \cdot \nabla_{in} V \times \nabla_{in} (pV^{5/3})$$

- The quantity $pV^{5/3}$ is conserved in ExB drift, so simple theory suggests that $pV^{5/3}$ is approximately constant in the plasma sheet.

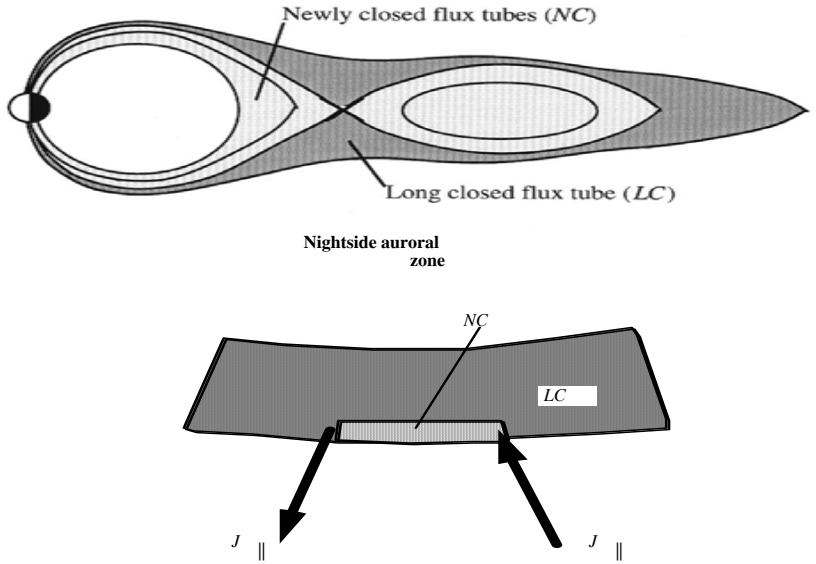

- Reconnection naturally creates new closed field lines with reduced $pV^{5/3}$
- That creates a current wedge

Problems with Near-Earth-Neutral-Line Model

- It doesn't naturally explain the fact that the auroral substorm begins with a brightening of the equatorwardmost arc, which apparently maps only to ~ 8 R_E.
- It doesn't naturally explain the violent changes in the plasma sheet near 8 R_E at substorm onset.
- NENL advocates explain this as the effect of the outflow from the reconnection impacting the strong-magnetic-field region near the Earth

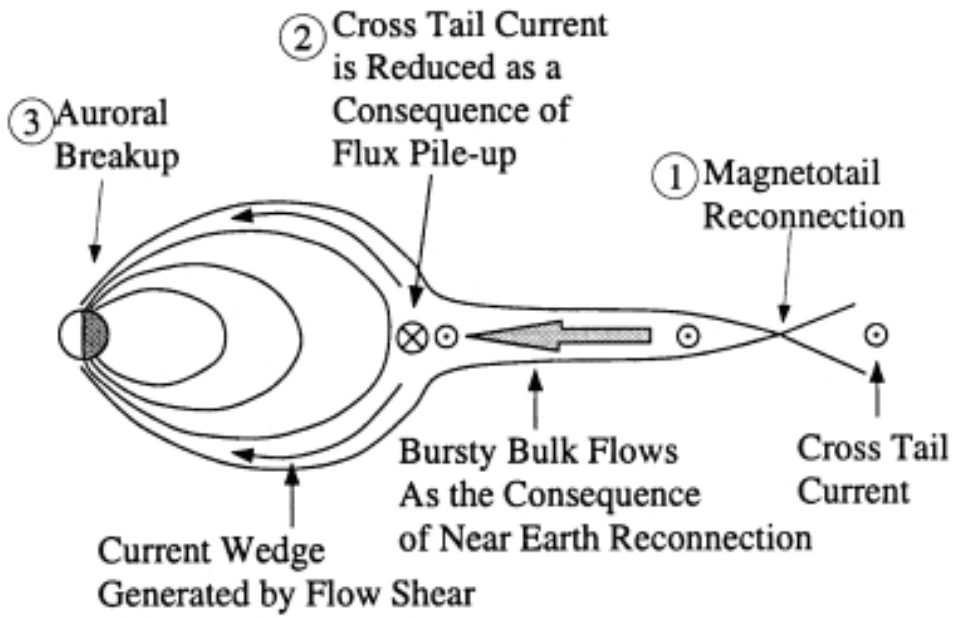

Tail-Current-Disruption Model

- Some small-scale process interrupts the cross-tail current at ~ 10 R_E, causing the field lines to dipolarize, slipping on the plasma.
  - An attempt has been made to identify the small-scale process, but without definitive success.
- The X-line forms later at ~ 25 R_E as a result.
- Equatorwardmost arc and 8 R_E turbulence occur on or near the field lines that undergo the slip/dipolarization/current-disruption.

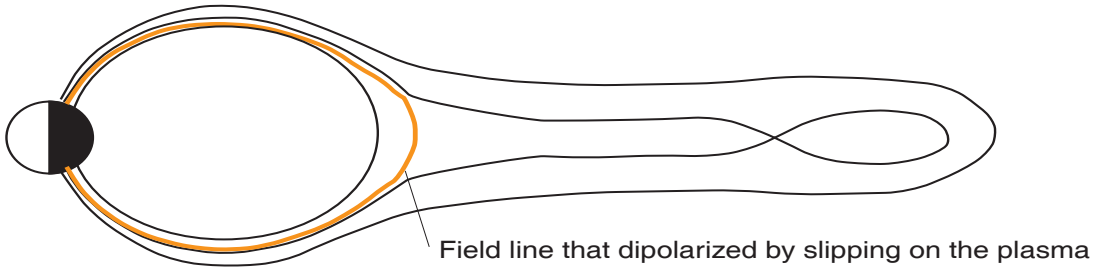

Tail-Current-Disruption Model– Strong and Weak Points

- Strong point:
  - Explains observations both near 8 R_E and near 25 R_E.
- Weak points:
  - Hasn't been made quantitative yet.

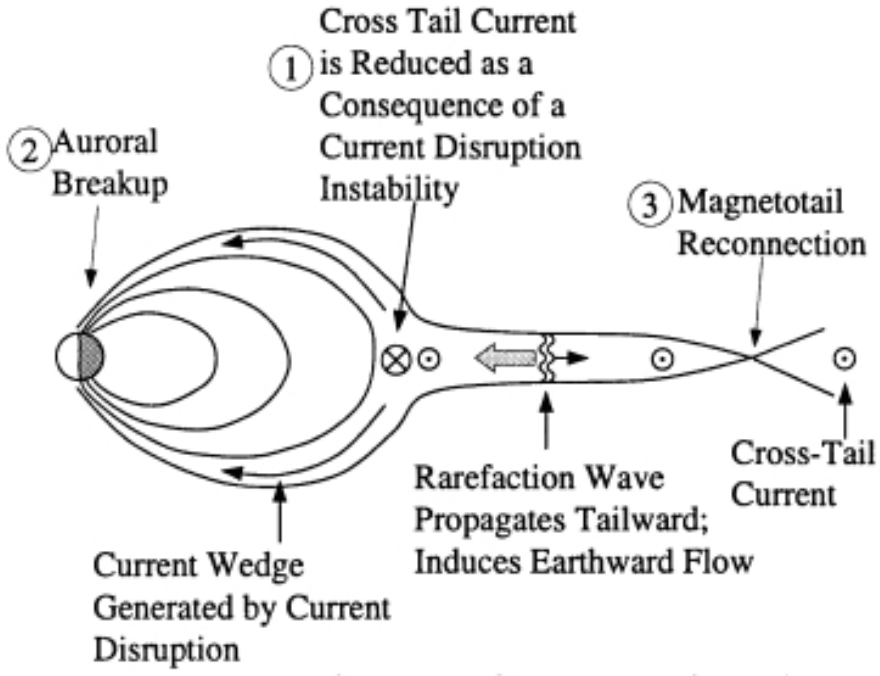

Competing Theories - THEMIS

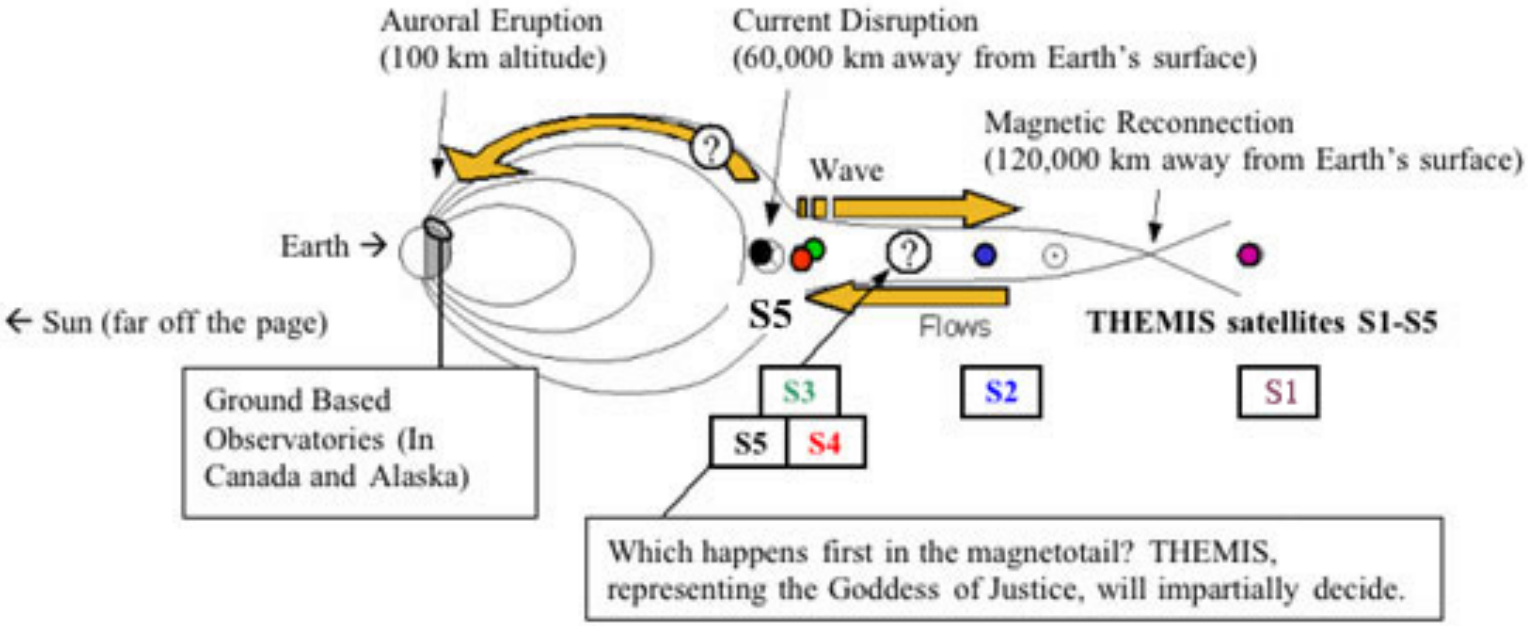

THEMIS website

Configurational Instability Model

- This model assumes that some global instability similar to ballooning occurs in the inner plasma sheet at substorm onset.
- Ballooning is a generalized form of interchange
  - Portions of adjacent field lines partly exchange positions.

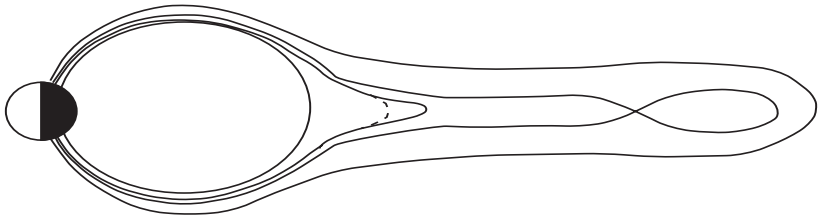

- That eventually leads to reconnection.
- Strong points:
  - MHD waves are observed near the inner edge of the plasma sheet near local midnight.
- Weak point:
  - Nobody has been able to construct a coherent theoretical picture based on this idea:
    - It is not clear whether the stretched inner plasma sheet is unstable to ballooning or anything else.
      - MHD ballooning is relatively simple theoretically, but the inner plasma sheet is near marginal stability for that.
      - Finite gyro-radius and other kinetic effects complicate the instability
        - » Theoretical picture is very unclear.

MHD Ballooning in the RCM-E

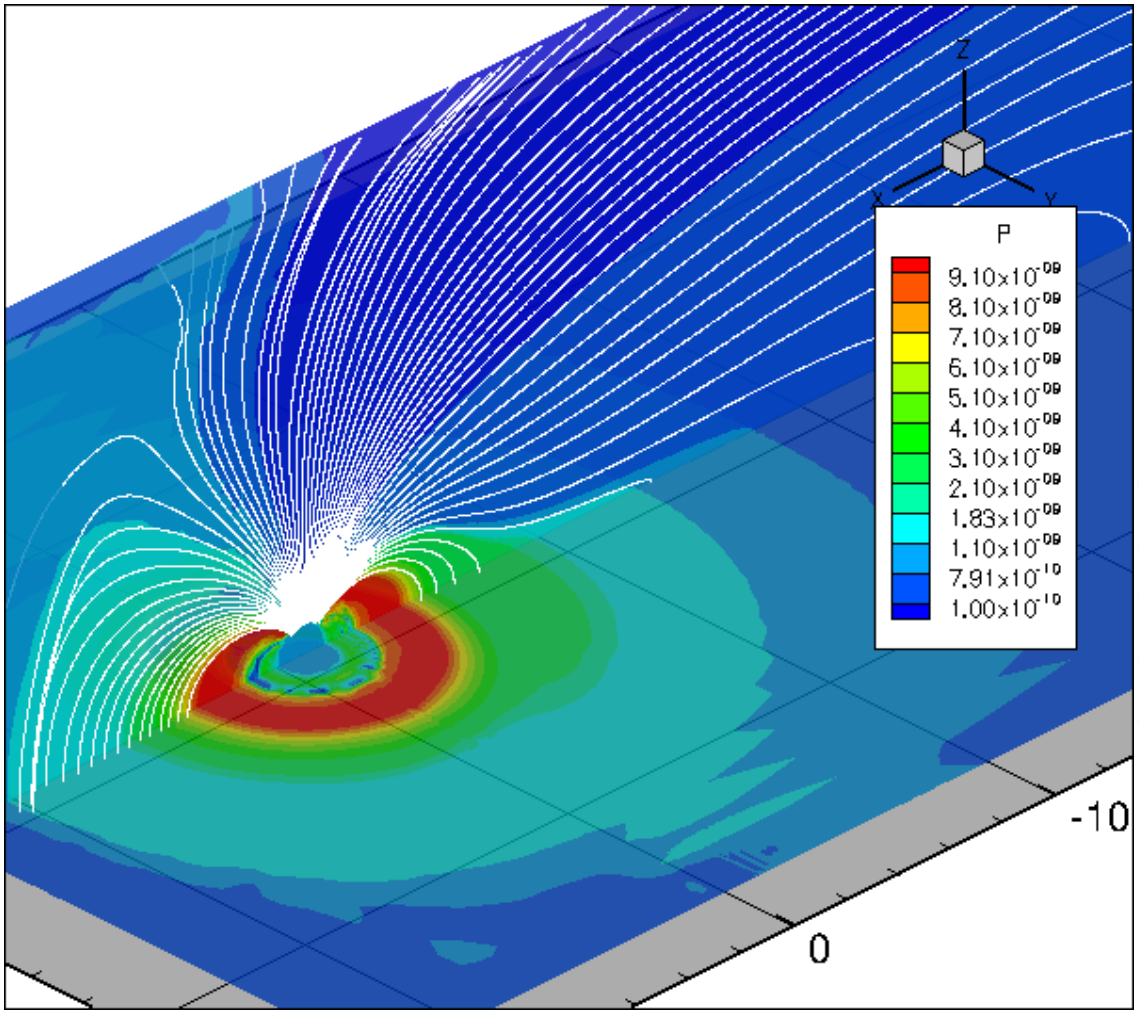

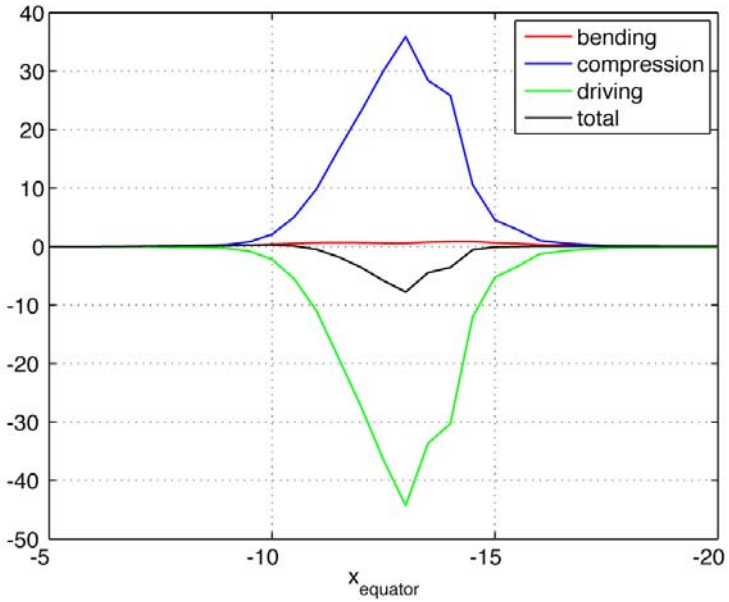

Azimuthal Drift Model

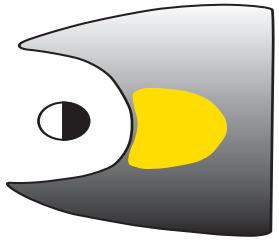

- The dawnside plasma-sheet ions may come from the low-latitude boundary layer and therefore have lower average energy than the duskside plasma-sheet ions
- In the absence of strong convection, gradient/curvature drift dominates the transport, and the duskside ions will run away from the dawnside ions, creating a low-plasma-pressure region in between.
  - That forms the substorm current wedge.
  - Model due to Lyons (JGR, 100, 19069, 1995)
- Advantage:
  - Explains substorm triggering by northward turning
- Disadvantage:
  - Hasn’t been worked out in any quantitative detail.

Comparative CME and Magnetosphere Phenomena

Pre-Eruption

- Flux cancellation for CMEs & flux buildup for substorms

Eruption

- Instability mechanisms for CMEs and substorms

Post-Eruption

- Heating on closed field lines
- Current sheets and blobs
- CME/plasmoid acceleration and propagation
- In-transit cooling and magnetic transfiguration

Particle Energization

- Reconnection and shock models

Sheath Phenomena

- Draping, turbulence, accretion and reconnection

From Siscoe, 2004

Pre-Eruption

- Forbes/Hughes/Bhattacharjee

Eruption

- Forbes/Hughes/Bhattacharjee/ Reeves

Post-Eruption

- Raymond/Golub/Korreck/Reeves/ Spence
- van Ballegooijen/Hughes
- Forbes/Siscoe/Goodrich/Raeder
- Owens/Crooker/Siscoe

Particle Energization

- Lee/Schwadron/Korreck

Sheath Phenomena

- Farrugia/Smith/Richardson/ Siscoe/Crooker

Similar CME and Substorm Eruption Scenarios

SUBSTORM \ CME		Directly Driven		Blocking-Release			Disequilib.
		Thermal Blast	Dynamo	Tether Release	Tether Straining R	Tether Straining B	Mass Loading
Drctly Drvn	IMF Connec.		●				
Blocking-Release	Recon. Inst.			●	●		
	Config. Inst.					●	
	Current. Inst.						
	Mass Exchng.						●
	MIC Inst.		●				
Dis-eqlb	Triggered. Diseqlib.						●

From Siscoe, 2004 - size of ‘dot’ corresponds strength of similarities.

Pressure-Balance Inconsistency

- Also called “pressure crisis”
- Two results from adiabatic drift theory:

$$pV^{5/3} = \frac{2}{3}\sum_s \eta_s \lambda_s$$

$$\left(\frac{\partial}{\partial t} + \mathbf{v}_D(\lambda, \mathbf{x}, t)\cdot\nabla\right)\eta_\lambda(\mathbf{x},t) = -\frac{\eta_\lambda(\mathbf{x},t)}{\tau_\lambda(\mathbf{x},t)}$$

- In the absence of loss by precipitation or charge exchange, the quantity $p_s V^{5/3}$, where p_s is partial pressure due to particles of type *s*, is constant along the drift path of a particle of that type.
- Is loss really negligible?
  - Electrons
    - Loss lifetimes for plasma-sheet electrons are ~ 1 hour, so loss is significant.
    - However, electrons carry only ~ 1/7 the plasma sheet pressure.
  - Ions
    - Precipitation loss is much slower for plasma-sheet ions than for electrons, because ion thermal velocities are much slower.
    - Charge exchange is very slow for $L > 6$.

Observed $pV^{5/3}$

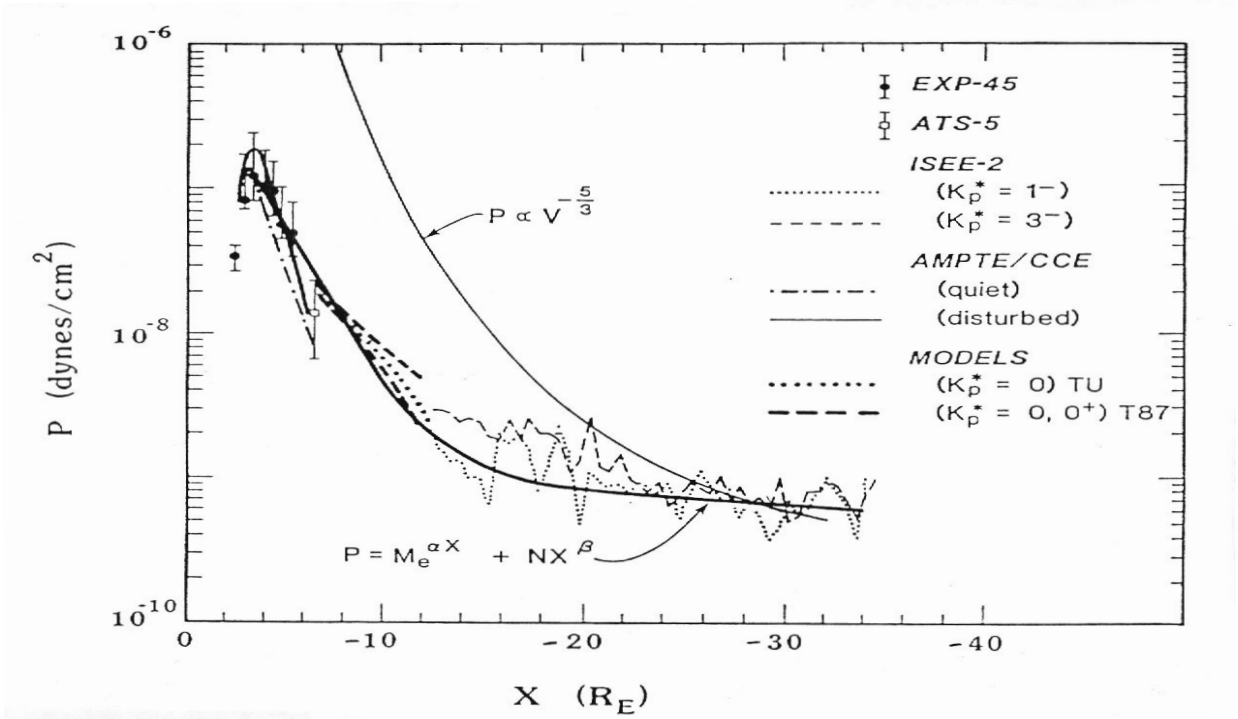

Comparison of observed plasma sheet particle pressure with curves $pV^{5/3}$=constant, with V estimated from Tsyganenko (1987) model. Adapted from diagram by Harlan Spence.

- $pV^{5/3}$ increases about a factor of 10 between X=-15 and X=-30

Pressure Balance Inconsistency and the Substorm Growth Phase

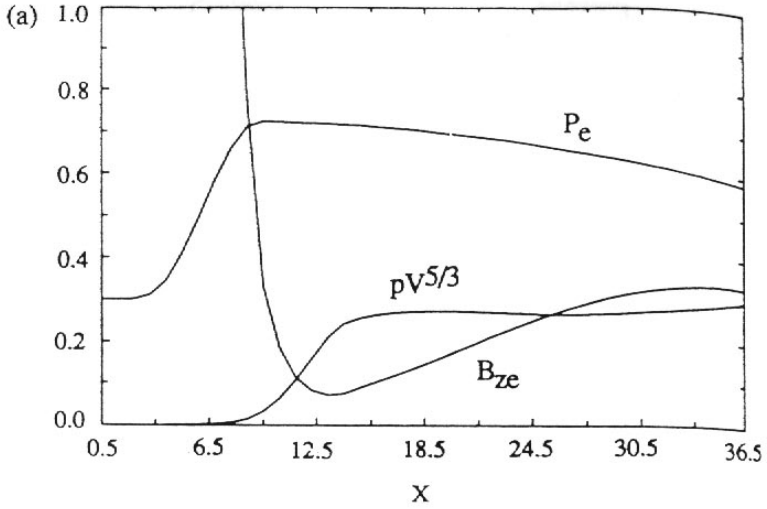

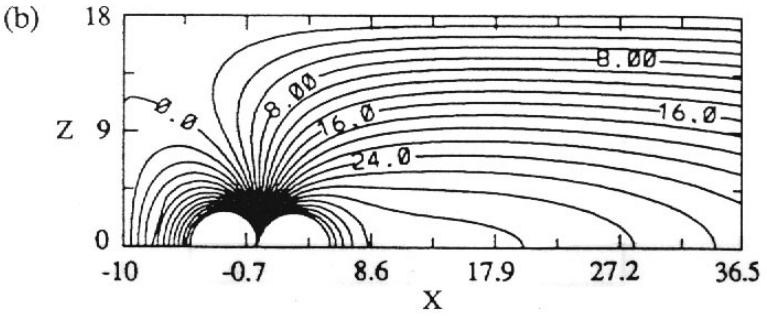

2D equilibria from Hau (JGR, 96, 5591, 1991)

Also confirmed in 3D using the RCM-E.

Summary on Pressure-Balance Inconsistency

- Adiabatic convection in the plasma sheet naturally leads to a highly stretched inner plasma sheet, with small B_z, thin current sheet, strong tail lobe field.
- When convection is very weak, this effect may be nullified by gradient/curvature drift out the sides of the tail, but that doesn't work for strong convection.
- Bursty bulk flows (BBFs)– probably mostly due to patches of reconnection–help to nullify the PBI effect, by producing low-$pV^{5/3}$ flux tubes.
- In times of strong convection, probably, BBF's aren't enough, and the inner plasma sheet becomes highly stressed over a wide region.
- Then the highly stressed plasma system breaks, creating a substorm expansion phase. That produces dipolarized, low -$pV^{5/3}$ flux tubes and releases the stress.
- I think we pretty much understand the substorm growth phase. The physics of the expansion phase is unclear.

Example

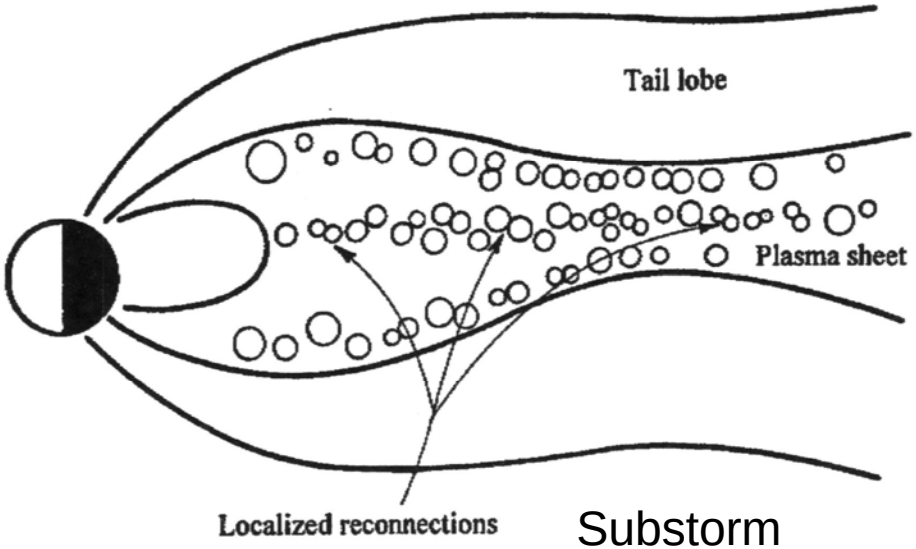

Substorm

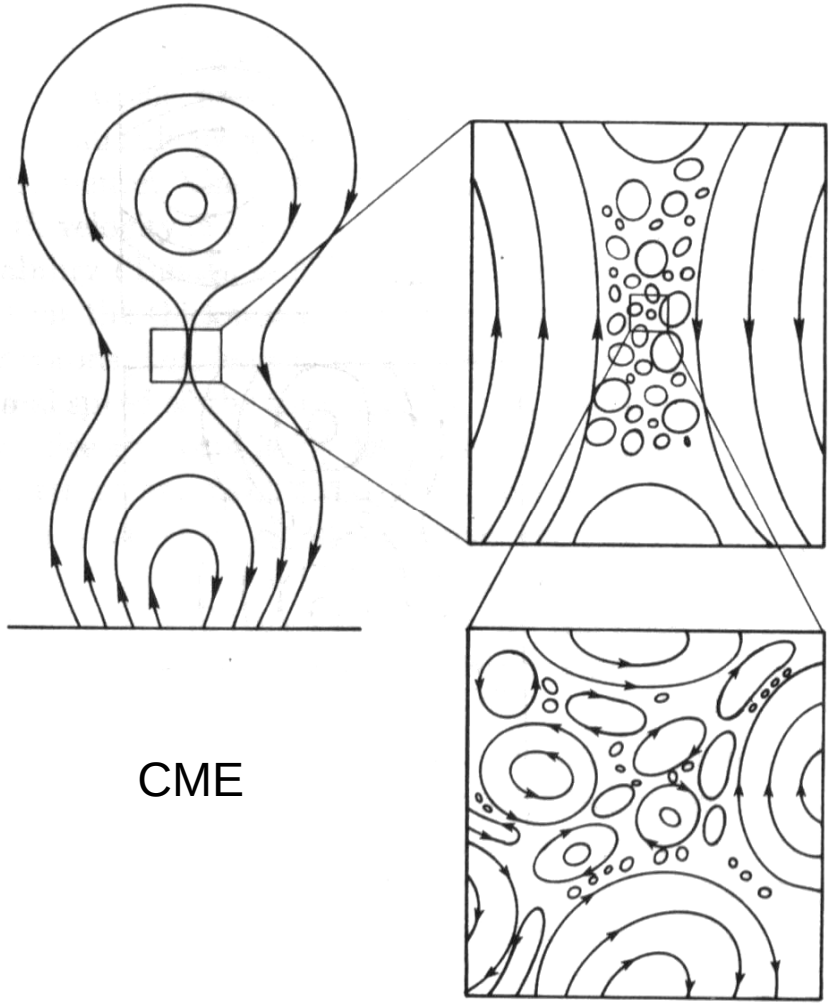

CME

From Siscoe, 2004

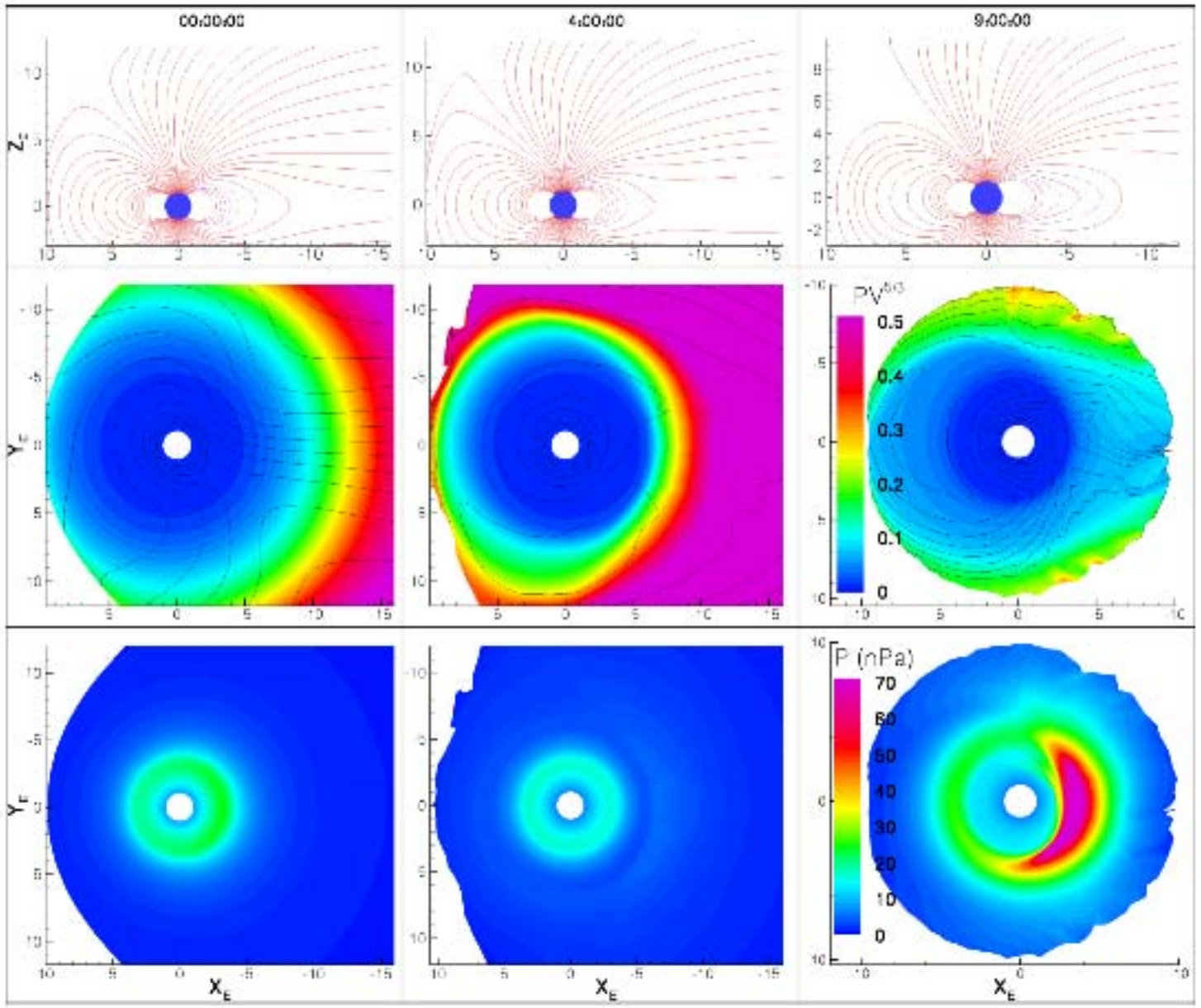
00:00:00
4:00:00
9:00:00
Z_E
Y_E
$PV^{2/3}$
0.5
0.4
0.3
0.2
0.1
0
P (nPa)
70
60
50
40
30
20
10
0
X_E

RCM-E Storm simulations

- In order to achieve a strong ring current inject, Lemon et al, artificially reduced the pV^{γ} at the RCM's tailward boundary in a limited local time region
  - This resulted in a strong ring current injection
- Kan et al [2007] estimated that if this pV^{γ} reduction is the result of reconnection, then the X-line should line at a tailward distnace between -15 and -25 R_E
- Similar channels on low pV^{γ} occur in the coupled RCM-LFM code

Reduced flux tubes in the coupled RCM LFM

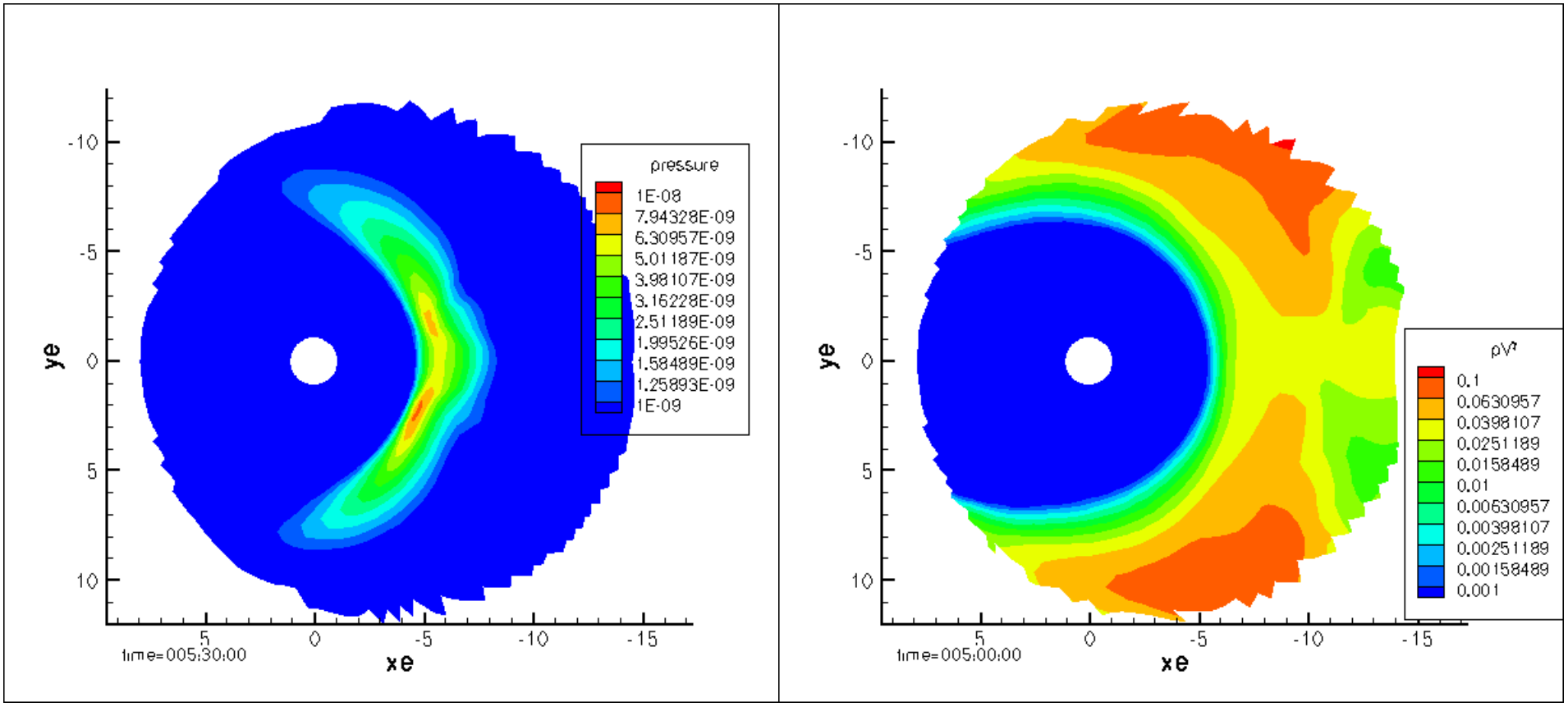

Some unanswered Questions

- What exactly is the physical process that we call a substorm?
  - Are all substorms alike?
  - Is there a single process that controls the physics of a substorm or is it a global process?
  - How similar is a CME to substorm?
- What is the relationship between storms and substorms?
  - Storm = Σ Substorms?
- What role does the ionosphere play?
- What are the processes that determine how energetic particles are accelerated/lost in the radiation belt during storms and substorms?
  - Did not talk about this subject

Take home message

- Both areas of research are very active with many basic unanswered questions.
  - Substorm physics is in need of some new approaches and interpretations.
- Numerical models are approaching a level of sophistication that quantitative predictions can now be done.
  - Coupled with the recent launch of the THEMIS mission, the next few years could see some significant advances in our understanding of storms and substorms.

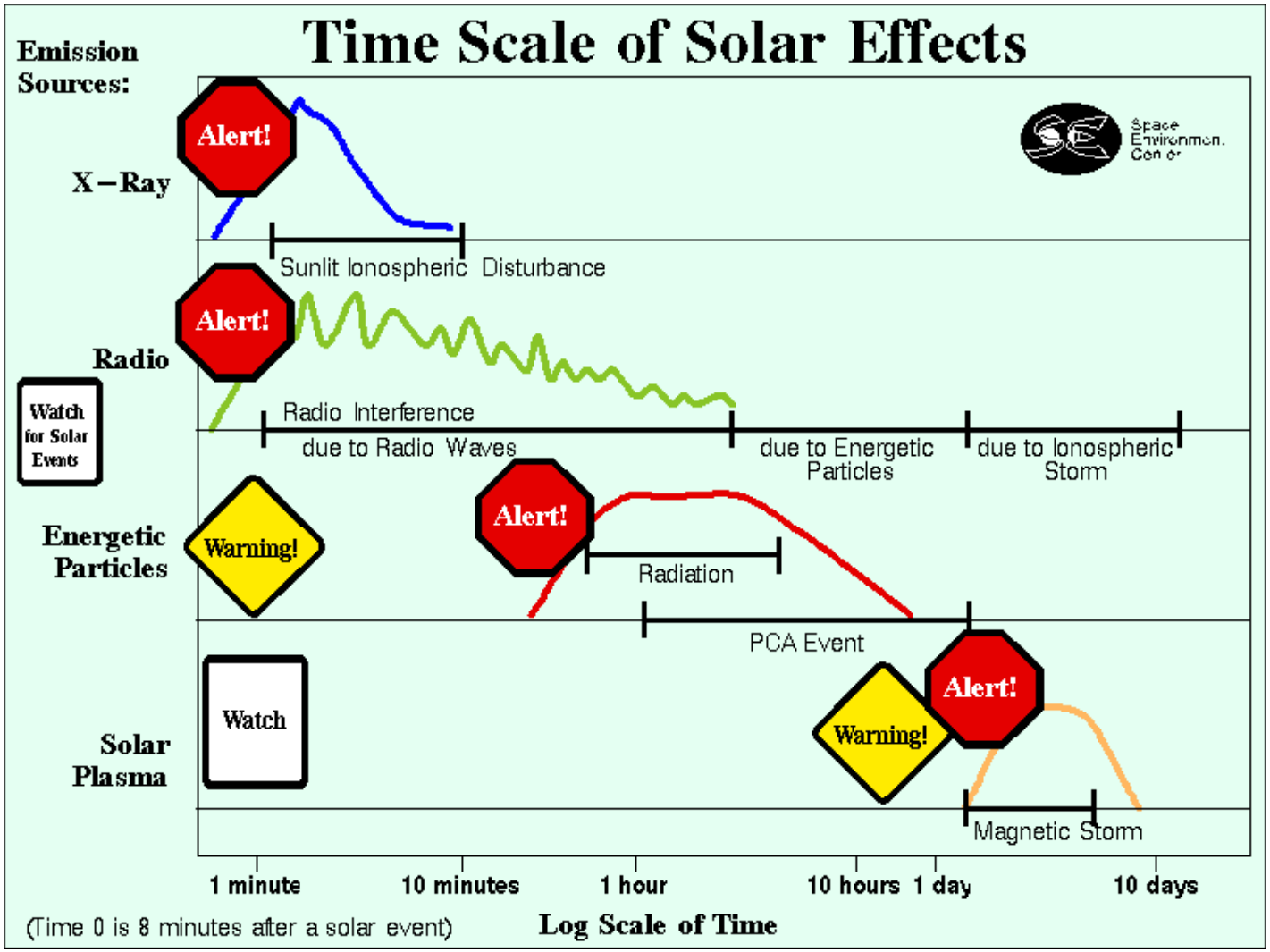

NOAA website

NOAA Space Weather Scales Š Geomagnetic Storm

Scale	Descriptor	Physical Measure	Average Frequency (1 cycle = 11 years)
G 5	Extreme	Kp=9	4 per cycle (4 days per cycle)
G 4	Severe	Kp=8, including a 9-	100 per cycle (60 days per cycle)
G 3	Strong	Kp=7	200 per cycle (130 days per cycle)
G 2	Moderate	Kp=6	600 per cycle (360 days per cycle)
G 1	Minor	Kp=5	1700 per cycle (900 days per cycle)

Source: NOAA SEC website

The Kp-index is a quasi-logarithmic scale that has a range from 0 to 9 and is directly related to the maximum amount of fluctuation (relative to a quiet day) in the geomagnetic field over a three-hour interval averaged over 13 several ground stations.